Daler *et al. Chem. Biol. Technol. Agric.* (2024) 11:108
https://doi.org/10.1186/s40538-024-00609-6

Chemical and Biological Technologies in Agriculture

RESEARCH

Open Access

Modulatory effects of selenium nanoparticles against drought stress in some grapevine rootstock/scion combinations

Selda Daler[1], Nesrin Korkmaz[2], Tuğba Kılıç[1], Harlene Hatterman-Valenti[3], Ahmet Karadağ[4] and Ozkan Kaya[3,5,6*]

Abstract

Background Drought is a significant abiotic stress that adversely affects plant growth, development, and metabolic processes, thereby reducing plant yield, quality, and production, and threatening global food security. In recent years, nanotechnology has emerged as a promising strategy to overcome the existing environmental challenges and has been tested on some plant species. But it is still awaiting investigation for grapevines. The aim of this study was to investigate the potential of selenium nanoparticles (Se-NPs) to modulate some morphological, physiological, and biochemical parameters in grapevine saplings (5 BB/Crimson Seedless, 41 B/Crimson Seedless, and 1103 P/Crimson Seedless) under drought stress conditions.

Results In the study, Se-NP solutions at different concentrations (0 (control), 1, 10, and 100 ppm) were applied by the spray method to wet the entire green surface of grapevine saplings grown under well-irrigated (90–100% field capacity) and drought stress (40–50% field capacity) conditions. Our results showed that 10 ppm Se-NP concentration had the most positive effect, 1 ppm concentration showed limited effects, and 100 ppm concentration led to toxic effects, especially when combined with drought conditions. Se-NP applications at 10 ppm concentration improved the growth parameters (leaf number, leaf area, root fresh and dry weight, shoot fresh and dry weight, etc.) and increased the SPAD index of grapevine saplings under both normal and drought conditions. Additionally, 10 ppm Se-NP applications improved the relative water content (RWC) and stomatal conductance values, proportional to the increases in protein content. On the other hand, under drought conditions, the drought index, leaf temperature, membrane damage index, hydrogen peroxide (H_2O_2) content, and malondialdehyde (MDA) levels significantly decreased as a result of 10 ppm Se-NP applications, showing an opposite trend. Furthermore, the levels of proline, total phenolics, and antioxidant enzymes (CAT, SOD, and APX) that rose significantly due to drought stress were reduced by 10 ppm Se-NP applications, which also helped to lessen the oxidative stress caused by the drought.

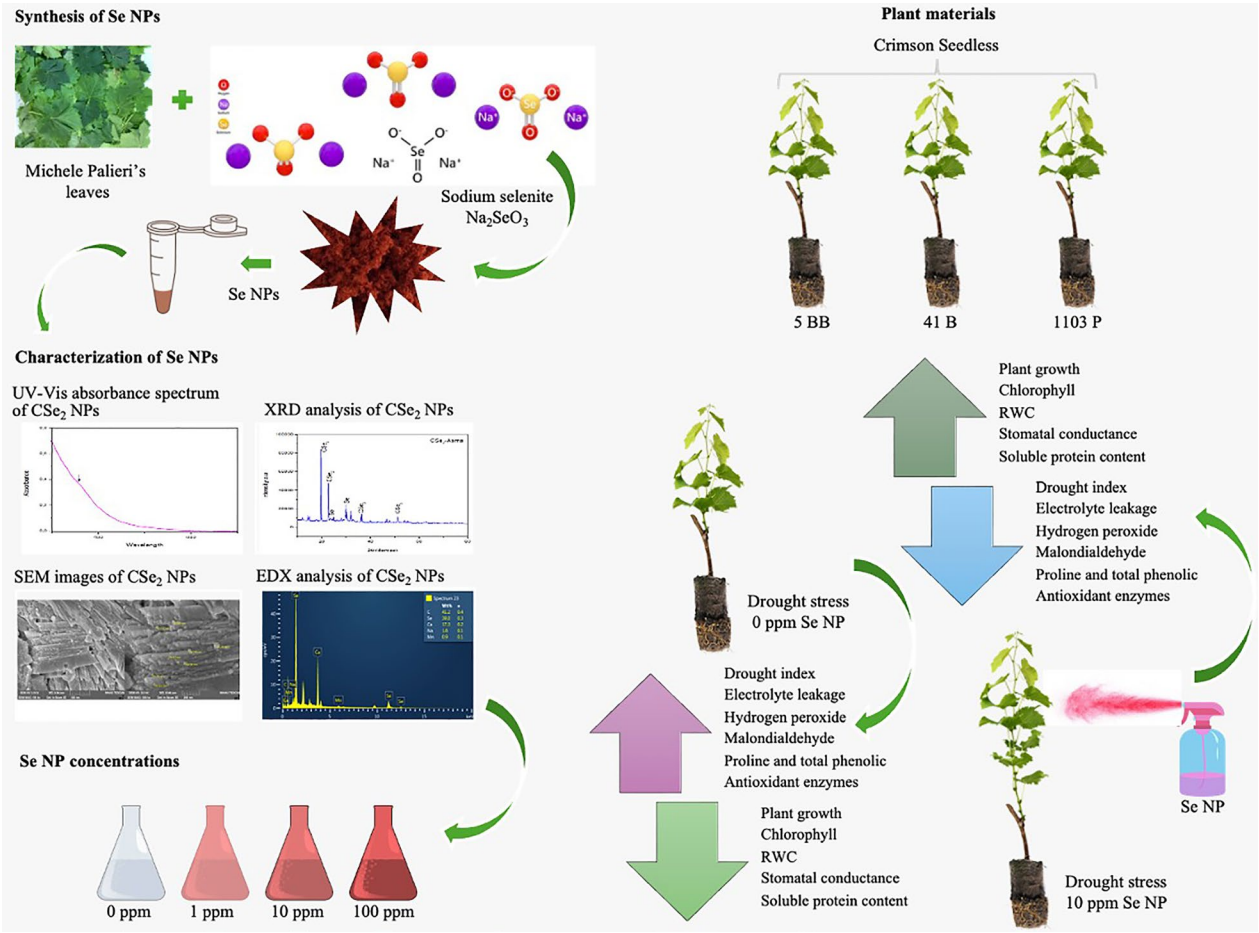
Conclusion The study concluded that foliar application of Se-NPs at 10 ppm significantly enhances drought tolerance in grapevine saplings by improving antioxidant defense, proline and protein accumulation, and overall growth, while lower concentrations are less effective and higher concentrations can cause phytotoxicity. These findings indicate that Se-NPs applications may hold promise not only for grapevines but also for mitigating drought stress effects and improving productivity in other economically important fruit species, warranting further exploration across diverse crop systems.

Keywords Crimson seedless, Drought stress, Grapevine rootstock, Se-NPs, *Vitis* spp.

*Correspondence:
Ozkan Kaya
ozkan.kaya@ndsu.edu; kayaozkan25@hotmail.com
Full list of author information is available at the end of the article

This is a U.S. Government work and not under copyright protection in the US; foreign copyright protection may apply 2024. **Open Access** This article is licensed under a Creative Commons Attribution 4.0 International License, which permits use, sharing, adaptation, distribution and reproduction in any medium or format, as long as you give appropriate credit to the original author(s) and the source, provide a link to the Creative Commons licence, and indicate if changes were made. The images or other third party material in this article are included in the article's Creative Commons licence, unless indicated otherwise in a credit line to the material. If material is not included in the article's Creative Commons licence and your intended use is not permitted by statutory regulation or exceeds the permitted use, you will need to obtain permission directly from the copyright holder. To view a copy of this licence, visit http://creativecommons.org/licenses/by/4.0/. The Creative Commons Public Domain Dedication waiver (http://creativecommons.org/publicdomain/zero/1.0/) applies to the data made available in this article, unless otherwise stated in a credit line to the data.

Graphical Abstract



Introduction

In recent years, potential effects of climate change include an increase in annual average temperatures leading to hot air waves and extreme high-temperature events, known as "global warming" [1]. Damages resulting from climate change and global warming can cause significant economic losses in plant species with a large production area and high economic value. The viticulture sector, with a production volume approaching 75 million tons in over 90 countries worldwide and a surface area of 7 million hectares, is among the major agricultural sectors that will be affected by drought [2]. Based on reports from the Intergovernmental Panel on Climate Change [3], the average global air and surface temperature is projected to rise between 1 and 4.5 °C, resulting in more severe drought events in many traditional viticulture regions, increasing the need for irrigation [3]. Water emerges as the most critical factor limiting plant productivity in agricultural systems, especially in arid and semi-arid climate regions [4]. Particularly in table grape cultivation, water deficiency adversely affects important parameters such as yield, berry size, and firmness. The cultivation cycle of table grapes encompasses spring, summer, and autumn seasons, when irrigation demand is highest [5]. This situation leads to the depletion of freshwater resources and an increasing global pressure on irrigation resources [1, 5]. Today, reducing water usage has become a necessity to promote sustainable management of viticulture [5]. Due to the increasing vulnerability of water resources in many viticulture regions, the physiological responses of grapevines to drought stress have attracted significant interest among

researchers [6]. Grapevines have developed various interconnected and highly complex mechanisms to cope with the adverse effects of drought [7]. Drought stress triggers numerous morphological (reduced leaf area, leaf number, increased root length, leaf senescence, early maturation, changes in growth stages, etc.), physiological (stomatal activity, photosynthesis, osmotic balance, transpiration, leaf water potential, water transport, etc.), and biochemical (antioxidant content, chlorophyll content, proline accumulation, hormonal content, secondary metabolites, etc.) responses in grapevines, leading them to develop adaptation mechanisms to withstand stress conditions [7, 8]. However, the developed defense mechanisms may not be sufficient to mitigate the harmful effects of ROS under prolonged drought stress conditions. Therefore, alternative approaches are needed to promote the plant defense system and enhance tolerance to drought stress.

Until now, various vineyard management strategies have been developed to improve water use efficiency in vineyards and reduce drought-induced stress damage in grapevines. These strategies include; dry farming conditions [9], deficit irrigation applications [10], the use of tolerant varieties [11] and rootstocks [12], mulching and cover crops [13], reducing the use of nitrogen-based fertilizers and certain training systems [14], and the use of remote sensing technologies to design more efficient irrigation programs [15]. These developed techniques are vital in mitigating the damage caused by both high temperatures and drought due to climate change. However, today, strategies to adapt viticultural practices to the challenges of climate change are based on innovative management techniques. Recent studies have highlighted nanotechnology (NT) as an effective strategy for mitigating the adverse effects of environmental stress and reducing crop yield and quality losses [16]. Although the use of NT in the agricultural industry is relatively new, nanoparticles (NPs), which form the basis of NT, have a wide potential for application in agricultural fields due to their distinctive physicochemical properties such as surface-to-volume ratios, size, and optical properties [17]. Research has shown that NP applications are an effective strategy for increasing tolerance to various environmental stress factors in plants and ensuring sustainability in agricultural areas [16, 18, 19]. On the other hand, selenium (Se), by acting as an antioxidant, can protect plants from oxidative damage and modulate the adverse effects of abiotic stresses on plants [20]. Indeed, Asghari et al. [21] found that Se-NPs at concentrations of 50 and 100 ppm improved the physiological and phytochemical properties of basil (*Ocimum basilicum* L.) under drought stress conditions. Besides, Ikram et al. [22] determined that foliar application of 10, 20, 30, and 40 Se-NPs to wheat under drought stress increased parameters such as plant height, shoot length, shoot fresh weight, shoot dry weight, root length, root fresh weight, root dry weight, leaf area, leaf number, and leaf length. Zahedi et al. [23] reported that SiO_2 NP, Se NP, and Se/SiO_2 NP at concentrations of 50 and 100 ppm improved the growth and yield parameters of strawberry grown under drought stress conditions. Djanaguiraman et al. [24] stated that Se-NP applications at concentrations of 0, 100, 250, and 500 ppm alleviated high-temperature stress damage in sorghum plants by increasing the activity of antioxidant enzymes, thereby inducing the antioxidative defense system. However, while the effectiveness of NPs in improving stress tolerance varies among plant species, the most effective concentration range also differs. Therefore, more research is needed to investigate the potential of NPs for use in agricultural areas, evaluate the advantages and potential disadvantages of their effects on plant growth and development, as well as biotic and abiotic stress tolerance in detail. Understanding the mechanisms of action of NPs is of great importance, especially for a plant species with a large production area and high economic value, such as grapevines. However, due to the lack of studies investigating the effects of Se-NPs on abiotic stress tolerance in grapevines in the current literature, significant gaps exist. In the reviews conducted, no study was found evaluating the effects of Se-NPs on the defence mechanisms developed against drought stress in grapevines.

From this perspective, the aims of the present study are as follows: i) to evaluate the effects of Se-NPs synthesized via green synthesis from grapevine leaves as an elicitor on the tolerance of grapevine saplings under drought stress conditions; ii) to investigate the modulatory effects of Se-NP applications at different concentrations on the morphological, physiological, and biochemical changes induced by drought stress in grapevine saplings; iii) to determine the optimal concentration ranges of Se-NPs for alleviating drought stress damage in grapevine saplings. This study, in this context, is the pioneering work evaluating the effects of green synthesized selenium nanoparticles at different concentrations on drought stress tolerance of grapevine saplings, determining the most effective concentrations, and providing the initial data regarding their impacts on the some morphological, physiological, and biochemical parameters related to the defense mechanisms developed against drought stress.

Materials and methods

Plant materials, experimental area, and establishment of the experiment

The present study was conducted between 2023 and 2024 at the laboratories of the Science and Technology

Application and Research Center (BİLTEM) and the existing research greenhouse and laboratories at the Faculty of Agriculture, Yozgat Bozok University. In the study, grapevine saplings of *V. vinifera* L. cv. Crimson Seedless (Emperor × C33–199) grafted onto 5 BB, 41 B, and 1103 P American rootstocks with varying drought tolerance were used (the relevant combinations have been previously tested, and no incompatibility issues were found). For the green synthesis of NPs, grapevine leaves of *V. vinifera* L. cv. Michele Palieri was utilized. The preparation stages for grafting and the grafting process were carried out at the grapevine grafting unit of the Department of Horticulture, Faculty of Agriculture, Yozgat Bozok University. After removing the rootstock and scion cuttings from the cold storage, they were soaked in fungicide-treated water for 48 and 24 h, respectively, followed by a thermotherapy treatment. Prior to grafting, the rootstocks underwent bud deblending and base trimming, while the scions were prepared for grafting by cutting them into a single bud. The grafting process was performed using the Omega (Ω) bench-grafting system, and immediately after grafting, the first paraffin application was carried out to ensure callus development at the graft union. After paraffining, a layering technique was applied, with a layer of moist pine sawdust and a layer of paraffined grafts placed alternatively in plastic crates. The layering crates were transferred to a growth chamber and maintained at 23 ± 2 °C temperature and 85–90% humidity for 21 days to facilitate graft union formation. Upon completion of the graft union formation, the grafted cuttings were removed from the crates, cleaned of sawdust using a compressor, and subjected to a second paraffin application to prevent moisture loss from the developed callus. Then, the grafted cuttings were transferred to the greenhouse for planting.

The experimental area where the study was conducted is a concrete-floored greenhouse with an area of ~ 200 m^2, a curved roof made of polycarbonate (PC) material, a 55% shade screen, a fan heater, a fan&pad system, and a ventilation system. Inside the greenhouse, there were rooting benches measuring 5 m in length, 1.20 m in width, 80 cm in height from the ground, and 20 cm in depth, where pots/containers could be placed. After being subjected to a rapid dip treatment with 2000 ppm indole butyric acid (IBA), the grafted grapevine saplings were planted in polyethylene (PE) pots measuring 11 × 11 × 22 cm (width × length × height) filled with an equal volume of sterile peat:perlite (1:1) mixture. Immediately after planting, the growing media containing the plants were irrigated daily with a full-strength nutrient solution recommended by Ollat et al. [25] for grapevine sapling cultivation, containing $Ca(NO_3)_2.4H_2O$ (2.5 mM), KH_2PO_4 (1.0 mM), KNO_3 (2.5 mM), $MnCl_2.4H_2O$ (9.2 µM), $MgSO_4.7H_2O$ (1.0 mM), Na_2MoO_4 (0.013 µM), $CuSO_4$ (0.5 µM), $ZnSO_4.7H_2O$ (2.40 µM), H_3BO_3 (46.4 µM), and NaFe(III)-EDTA (45 µM). The pH of the solution was adjusted to 6.5, and the irrigation amount was based on a 30% drainage rate until the application of drought stress (for three months). During the vegetation period, the greenhouse environment was maintained at 25 ± 5 °C temperature, 40 ± 10% relative humidity, and natural day length conditions using the heating and fan&pad systems to promote root and shoot development in the grafted saplings. Single-bud cuttings were used to prepare the grafted grapevine saplings, allowing the development of a single shoot. Approximately 8 weeks after planting, grapevine saplings exhibiting similar characteristics in terms of stem diameter and leaf area were selected and transferred to 2.5 L polypropylene (PP) containers measuring 12.5 × 12.5 × 20 cm filled with a soil:peat:perlite (1:1:1) mixture.

Green synthesis of nanoparticles: collection and extraction of leaf samples

Grapevine leaves were utilized as the reducing agent for the green synthesis of NPs. The grapevine leaves were harvested in June during the early stages of the growth period. For this purpose, the first five leaves from the apical part of each shoot were removed. The harvested leaves were subjected to drying in an appropriate environment, away from direct sunlight, to equalize their moisture levels. To obtain leaf extracts, the dried grapevine leaves were washed with pure water, dried, and then interacted with liquid nitrogen, resulting in their fragmentation into small pieces. 30 g of the fragmented leaf sample was extracted for 1 h at 60 °C in 100 ml of distilled water using a magnetic stirrer. After cooling to room temperature, the solution was centrifuged at 3500 rpm for 15 min and then filtered through a Whatman No. 1 filter paper to obtain the plant extract [26]. The obtained leaf extracts were stored at + 4 °C and utilized for the synthesis of Se-NPs.

Synthesis and characterization of selenium (Se) nanoparticles

In this study, commercial sodium selenite (Na_2SeO_3) (CAS: 10,102–18-8) from Sigma was utilized as the Se source. The synthesis of Se-NPs was carried out based on the synthesis method of Fardsadegh et al. [27]. A 10 mM Na_2SeO_3 solution was prepared by dissolving 0.263 g of Na_2SeO_3 in 100 ml of deionized water. To the prepared 15 ml stock solution, 5 ml of leaf extract was added, and

precipitation was attempted for 4 min under 800 W conditions using a microwave synthesis device (flexiWAVE, Milestone Srl, Milan, Italy). Then, the mixture was centrifuged at 8.000 rpm, and the supernatant was discarded. The remaining precipitate was dried in a drying oven at 60 °C for characterization [27]. The obtained nanoparticles were characterized using UV–Vis (ultraviolet–visible spectrophotometer), XRD-powder (X-ray diffraction), SEM (scanning electron microscopy), and EDX (energy-dispersive X-ray spectroscopy) techniques. The characterization processes were conducted through service procurement from BILTEM laboratories.

- ***UV–Vis analysis:*** During the green synthesis reaction, UV–Vis spectroscopy was generally performed on solutions taken from the solution to measure molecules or inorganic ions and complexes present.
- ***XRD-powder analysis:*** X-ray diffraction applied to powder samples allowed the determination of the crystalline structure as well as the necessary values for calculating the average particle size. The XRD analysis of Se samples was conducted at the Science and Technology Application and Research Center of Yozgat Bozok University.
- ***SEM analysis:*** High-resolution imaging of powder samples at high magnifications enabled the acquisition of surface images, providing information about the number, size, and morphology of small Se nanoparticles, as well as insights into the chemical composition of the material. SEM images of Se samples were obtained at the Central Research Laboratory of Bartın University.
- ***EDX analysis:*** This analysis was utilized for quantitative chemical analysis by taking advantage of the energies of the elements. In our study, EDX analysis was performed to obtain information about the elemental composition and purity of the Se samples. The EDX analyses of Se samples were conducted at the Central Research Laboratory of Bartın University.

Se-NP and drought stress applications

Previous studies have indicated that the application of NPs prior to stress treatment has led to a significant improvement in the physiological processes associated with stress [21, 23]. In this study, therefore, Se-NPs were applied before inducing drought stress. The Se-NPs obtained through the green synthesis method were considered pure, and initially, 1000 ppm stock solutions were prepared from these synthesis products. Then, these stock solutions were diluted to concentrations of 1, 10, and 100 ppm. For the control groups, distilled water was used. After transferring the plants to pots, Se-NP solutions at 0, 1, 10, and 100 ppm were sprayed evenly on the leaves, using 25 ml of solution per plant [24]. According to the literature, repeated elicitor applications are more effective and should be applied at certain intervals [23]. Therefore, in this study, Se-NPs were applied three times at one-week intervals. Approximately four weeks after the Se-NP applications, the saplings were subjected to drought stress according to the method described by Cochetel et al. [28]. Drought stress was applied at two different levels: control (90–100% field capacity) and limited irrigation (40–50% field capacity) [22]. The daily water loss in each pot was determined using the following formula based on the gravimetric substratewater content (GSWC) measurement method, utilizing a representative cultivation medium sample [29]:

$$\begin{aligned}\mathrm{GSWC}\ (\%) = &\left(\text{wet weight of the substrate}\right.\\ &\left.-\ \text{dry weight of the substrate}\right)\\ &/\left(\text{dry weight of the substrate}\right)\times 100.\end{aligned}$$

Throughout the experiment, the weight and moisture content of the substrate were monitored daily during the drought stress application period (for 30 days) to maintain the desired moisture levels. Water was supplemented daily at specified ratios until harvest. Additionally, all plants received full-strength nutrient solution [25] daily until harvest.

Morphological, physiological, and biochemical analyses

After the total 120-day cultivation period, covering May to August, the experiment was terminated. To determine the differences between treatments, morphological (degree of physical damage, leaf number, leaf area, shoot length, shoot fresh weight, shoot dry weight, shoot dry matter ratio, root length, root fresh weight, root dry weight, and root dry matter ratio), physiological (chlorophyll content, leaf relative water content, stomatal conductance, leaf surface temperature, and membrane damage index), and biochemical (proline content, total phenolic content, hydrogen peroxide content, lipid peroxidation, soluble protein content, superoxide dismutase "SOD", catalase "CAT", and ascorbate peroxidase "APX" antioxidant enzyme activities) parameters were analyzed.

Morphological analyses

At the end of the experiment, morphological parameters of the grapevine saplings' roots, shoots, and leaves were examined using samples taken either during or immediately after, depending on the analysis to be performed.

Degree of physical damage: Observations related to chlorosis damage on the saplings' leaves were evaluated based on the 1–5 scale reported by OIV [30]: 1—no chlorosis (dark green leaves); 2—slight chlorosis (interveinal areas light green); 3—moderate chlorosis (main veins green, interveinal areas yellow); 4—severe chlorosis (yellow leaves with less than 10% necrosis); 5—very severe chlorosis (yellow leaves with more than 10% necrosis). The degree of physical damage was calculated as the drought index percentage using the following formula according to the 1–5 scale values:

Drought index (%) = Σ(leaf × scale value) / (total leaves × highest scale value) × 100.

Leaf number: Starting from the first fully expanded leaf at the shoot apical, all leaves were counted towards the basal, and the average number of leaves per shoot was determined.

Leaf area: The size of at least three mature leaves from the middle third of the shoots for each replicate was measured using a leaf area meter (ADC BioScientific Area Meter AM-300), and the average values were recorded in cm^2.

Shoot length: The distance from the shoot apical to the basal was measured using a ruler, and the averages were recorded in cm.

Shoot fresh weight: The fresh weights of the shoots were weighed using an analytical balance with a precision of 0.0001 g, and the averages were expressed in g.

Shoot dry weight: After determining the fresh weights, the shoots were placed in an air-circulating oven at 65 °C for 72 h. Then, their dry weights were weighed using an analytical balance with a precision of 0.0001 g, and the averages were determined in g.

Shoot dry matter ratio: The shoot dry matter ratio was calculated as a percentage by dividing the shoot dry weight by the shoot fresh weight, and the averages were recorded.

Root length: The distance between the emergence points and the end point of the longest root on the saplings was measured using a ruler, and the averages were determined in cm.

Root fresh weight: The fresh weights of the roots were weighed using an analytical balance with a precision of 0.0001 g, and the averages were recorded in g.

Root dry weight: After determining the fresh weights, the roots were placed in an air-circulating oven at 65 °C for 72 h. Then, their dry weights were weighed using an analytical balance with a precision of 0.0001 g, and the averages were determined in g.

Root dry matter ratio: The root dry matter ratio was calculated as a percentage by dividing the root dry weight by the root fresh weight, and the averages were recorded.

Physiological analyses

The physiological characteristics of grapevine leaves were examined either immediately before uprooting the saplings from their growing medium or right after harvest, depending on the analysis to be performed.

Chlorophyll content: Two regions near the main vein of five leaves from each replicate were measured using a portable chlorophyll meter (Konica Minolta SPAD-502), and the average values were expressed in SPAD units [31].

Leaf relative water content (RWC): According to the method of Yamasaki and Dillenburg [32], the relative water content (RWC) of three leaves from each replicate was calculated as a percentage using the following formula, utilizing the fresh weight (FW) measured immediately after harvest, the saturated weight (SW) determined after soaking in pure water for 6 h, and the dry weight (DW) determined after drying in an air-circulating oven at 80 °C for 24 h:

$$\mathrm{RWC}\ (\%) = \left[\left(\mathrm{FW} - \mathrm{DW}\right) / \left(\mathrm{SW} - \mathrm{DW}\right)\right] \times 100$$

Stomatal conductance: For three leaves from each replicate, the reading sensor of the porometer (SC^{-1} Leaf Porometer, Decagon, Pullman, WA) was placed on the interveinal areas of the lower leaf surface, and measurements were taken. The obtained values were recorded in mmol m^{-2} s^{-1}.

Leaf surface temperature: The interveinal areas of three leaves from each replicate were measured using a leaf porometer, which can also measure leaf temperature values, and the obtained values were recorded as °C.

Membrane damage index: The membrane damage index was calculated by measuring the electrolyte leakage (EL) from the cells [33]. Three discs with a diameter of 6 mm were punched from three leaves of each replicate using a cork borer and soaked in 20 ml of deionized water for 4 h. The EC_1 values were measured using an EC meter (Jenway 470 condimeter). The same discs were then incubated at 100 °C for 10 min, and the EC_2 values of the solutions were measured. The membrane damage index (MDI) was calculated as a percentage (%) of EL using the following formula:

$$\mathrm{MDI} = (Lt - Lc/1 - Lc) \times 100$$

$$\left(Lt : EC_1/EC_2 \text{value of the leaf under drought stress;}\right.$$
$$\left.Lc : EC_1/EC_2 \textit{ value of the control leaf}\right).$$

Biochemical analyses

Immediately after uprooting the saplings at the end of the experiment, samples were taken from the fourth leaves of the grapevine saplings and stored at −80 °C in an ultra-deep freezer until the analyses were performed.

Proline content Proline content was determined according to the procedure applied by Bates et al. [34]. Leaf samples (~ 0.5 g) were homogenized in 7.5 ml of 3% sulfosalicylic acid. The homogenates were centrifuged at 6000 rpm for 10 min. Then, 2 ml of the supernatant was taken and mixed with 1 ml of glacial acetic acid and 1 ml of acid ninhydrin solution, followed by incubation at 100 °C for 1 h. After incubation, the tubes were cooled in an ice bath to stop the reaction. 4 ml of toluene was added to the tubes and mixed usin^{-1}g a vortex. The upper phase was collected, and the absorbance was measured at 520 nm using a UV spectrophotometer (Perkin Elmer Lambda 25). Toluene was used as a blank, and calculations were made using a calibration curve prepared with a proline standard, expressed as µmol g.

Total phenolic content The extraction process for determining the total phenolic content was performed according to the method of Kiselev et al. [35]. Approximately 1 g of leaf samples were weighed, and 10 ml of ethanol was added for homogenization. The homogenized samples were incubated at 50 °C for 30 min and then centrifuged at 9000 rpm for 10 min. The resulting supernatant was transferred to a new tube, and the ethanol was evaporated using an evaporator. After complete evaporation of ethanol, the remaining content in the tube was dissolved in 1 ml of methanol. The total phenolic content of the leaves was determined using the Folin–Ciocalteu colorimetric method according to Singleton and Rossi [36]. Absorbance values were measured at 765 nm using a UV spectrophotometer, and the results were calculated as gallic acid equivalents (GAE) in mg g^{-1} using a standard curve prepared with gallic acid solution.

Hydrogen peroxide (H_2O_2) content Approximately 0.5 g of leaf tissue was homogenized in 7.5 ml of cold 0.1% trichloroacetic acid (TCA), and the obtained homogenate was centrifuged at 12,000 rpm for 15 min. Subsequently, 0.5 ml of the supernatant was taken and mixed with 0.5 ml of 10 mM KH_2PO_4 buffer (pH: 7.0) and 1 ml of 1 M potassium iodide (KI) solution. Absorbance was measured and recorded at 390 nm. The results were calculated as the amount of H_2O_2 per gram of tissue (µmol g^{-1}) by comparing with a standard curve [37]. To prepare the standard curve, 0, 3, 6, 7.2, 10.8, 14.4, and 18 µg of H_2O_2 solution were transferred to separate Eppendorf tubes. The volume was adjusted to 1 ml with 10 mM KH_2PO_4 buffer (pH: 7.0). Then, 1 ml of 1 M KI was added to each tube. Absorbance values were read against a blank at 390 nm, and the results were recorded as µmol g^{-1}.

Lipid peroxidation Lipid peroxidation was determined according to the method of Lutts et al. [38]. Approximately 0.5 g of leaf sample was homogenized in 10 ml of 0.1% TCA, and the homogenate was centrifuged at 9000 rpm for 20 min. 1 ml of the resulting supernatant was mixed with 4 ml of 20% TCA solution containing 0.5% thiobarbituric acid (TBA). The reaction was carried out by incubating the mixture at 95 °C for 30 min and then stopped by placing the tubes in an ice bath. Absorbance values were measured spectrophotometrically at 532 and 600 nm. The MDA content was determined as nmol g^{-1} by substituting the obtained values into the formula:

$$\mathrm{MDA} = \left[(A532 - A600) \times \text{ Extract volume } (ml)/155\, mM/cm \times \textit{Sample amount}\left(mg\right)\right]$$

Soluble Protein Content The soluble protein content was determined using the method described by Bradford [39]. 50 mg of Coomassie Brilliant Blue G-250 was dissolved in 25 ml of 95% ethanol by heating. The prepared solution was mixed with 50 ml of 85% phosphoric acid and filtered using Whatman No. 1 filter paper. The final volume was adjusted to 500 ml with ddH2O to prepare the Bradford Coomassie Blue dye. The prepared dye was read at 595 nm against a blank to ensure its stability for the experiment. Bovine serum albumin (BSA) solutions were prepared at specific concentrations to create standard solutions. All standard solutions were read in a UV spectrophotometer, and their absorbance was obtained. A standard curve was plotted based on these values. 100 µl of enzyme extract was added to glass tubes, and 4.9 ml of Bradford solution was added and vortexed rapidly. The mixture was incubated for 10 min at room temperature in the dark and then read against a blank at 595 nm using a UV spectrophotometer. The obtained absorbance values were recorded, and their averages were calculated. The protein concentrations for each sample were determined using the standard curve.

Antioxidant Enzyme Activities For this purpose, approximately 1 g of leaf samples were homogenized in 4 ml of 50 mM K-phosphate buffer solution (pH: 7.0) containing 2 mM Na_2EDTA and 1% PVP. The obtained homogenates were centrifuged at 9000 rpm for 10 min at 4°C. The resulting supernatant was used to determine enzyme activities. Due to the ex vivo instability and short half-life of APX, 2 mM ascorbate was added to the extraction buffer in the APX analysis to preserve the compound's structure.

Superoxide Dismutase (SOD; EC 1.15.1.1) Enzyme Activity The method is based on the spectrophotometric determination of the inhibition of the photochemical reduction of nitro blue tetrazolium (NBT) to blue-colored formazan by superoxide radicals by the SOD enzyme [40]. The reaction mixture (3 ml) contains 50 mM KH2PO4 (pH: 7.8), 13 mM methionine, 63 µM NBT, 13 µM riboflavin, and 0.1 mM EDTA. For activity measurement, 2.58 ml of the above reaction mixture without riboflavin was added to a 3 ml spectrophotometer cuvette, and 30 µl of enzyme extract was added. The reaction was initiated by adding 390 µl of 13 µM riboflavin solution and mixing, followed by immediate placement under a white light source. The tubes were kept under the light source for 15 min, and the reaction was stopped by turning off the light source. The intensity of NBT color development was read against a blank at 560 nm within 15 min. The blank consisted of the same procedure without the enzyme sample. The amount of enzyme causing 50% inhibition of NBT reduction observed at 560 nm was considered as one enzyme unit, and the values were presented as U mg^{-1} protein [41].

Catalase (CAT; EC 1.11.1.6) Enzyme Activity The method applied by Gong et al. [42] was used. This method is based on monitoring the absorbance change at 240 nm while catalase catalyzes the conversion of H2O2 to oxygen and water. First, a standard curve was prepared to determine the amount of H2O2 decreasing in the reaction. To prepare the standard curve, 0.15, 0.3, 0.45, 0.6, 0.75, 0.9, 1.05, 1.2, 1.35, and 1.5 ml of 5 mM H2O2 solution were added to 3 ml spectrophotometer cuvettes, and the volumes were adjusted to 1.5 ml with ddH2O. Then, 1.47 ml of 103.5 mM KH2PO4 and 30 µl of ddH2O were added to each tube. The absorbance at 240 nm was read against a blank in a UV spectrophotometer, and a standard curve was obtained using the absorbance values corresponding to the µM H2O2 values. For activity measurement, 1.475 ml of 103 mM KH2PO4 buffer and 1.5 ml of 40 mM H2O2 substrate solution were added to 3 ml spectrophotometer cuvettes, followed by the addition of 25 µl of enzyme extract. The absorbance values were read against a blank at 240 nm wavelength in a UV spectrophotometer at 1-min intervals for 3 min, and the decrease in absorbance per minute was calculated from the interval where the absorbance decreased linearly. These average absorbance values were converted to µmol amounts of H2O2 using the standard curve. The amount of enzyme that decreased the absorbance by 1 µmol in 1 min at 25°C was considered as 1 enzyme unit, and the results were recorded as enzyme units per mg of total protein (U mg^{-1} protein).

Ascorbate Peroxidase (APX; EC 1.11.1.11) Enzyme Activity The method is based on the principle of measuring the oxidation of ascorbate by the enzyme in the sample at 290 nm absorbance using a UV spectrophotometer. The reaction mixture (2 ml) consisted of 50 mM K-phosphate buffer solution (pH: 7.0), 0.5 mM ascorbic acid, 1 mM Na2EDTA, 0.1 mM H2O2, and 50 µl of enzyme extract. The oxidation of ascorbate was initiated by adding the enzyme extract to the reaction mixture, and the reaction was monitored for 3 min. The amount of oxidized ascorbate was calculated using the extinction coefficient (2.8 mM/cm). The amount of ascorbate oxidized by the enzyme per minute per mg of total protein was considered as 1 unit, and the results were recorded as U mg^{-1} protein [43].

Experimental design and data evaluation

All experiments were conducted using a three-factor completely randomized design (CRD). Three replicates (each replicate containing nine plants) were used for each parameter corresponding to each experimental

group. The numerical data obtained were recorded using Microsoft 365 Excel. Since the experiment was set up as a three-factor trial, with the first factor being rootstock/scion combinations, the second being the irrigation regime, and the third being NP concentrations, the data were subjected to three-way analysis of variance (three-way ANOVA) using the IBM SPSS vrs. 22.0 package program (IBM, Armonk, NY, USA) to determine whether there was an interaction between the independent variables. For post hoc comparisons, mean separation among treatments was obtained at a 5% probability level ($p \leq 0.05$) using Duncan's multiple range test. The data were reported as mean values with corresponding standard deviations (SD). Correlation analysis was performed using the SRPLOT online platform (https://www.bioinformatics.com.cn/en accessed on January 21, 2024) to evaluate the relationships between the studied traits. Additionally, principal component analysis (PCA) was conducted explaining better the relationships among the treatments. Furthermore, a hierarchical clustering heatmap was generated to visualize and associate the relationships and intensities between the factors and the studied traits.

Results

Characterization of nanoparticles

Although nanoparticles could be easily synthesized via the green synthesis method, the experiment was set up three times to obtain a sufficient amount of product for characterization and other studies due to the low yield of the obtained product. For UV–Vis spectrophotometer results of Se-NPs, a significant color change from green to dark red was observed in the solution after the reaction (Fig. 1A). This color change is evidence of the formation of Se-NPs in the medium. The UV–Vis spectrum analysis of Se-NPs was monitored by measuring in the wavelength range of 200–400 nm with a scanning speed of 1.856 nm/min using a Shimadzu instrument. In Fig. 1A, a slight trend around 357 nm, which is not very sharp, is observed. Regarding XRD results of Se-NPs, the XRD spectrum prepared from selenium NPs is shown in Fig. 1B. The sharp peak points support the formation of well-crystallized CSe_2-NPs. These sharp peak points were related to the peak points centered at 23.5°, 29.2°, 41.4°, 43.3°, 45.4°, 52.5°, 55.7°, and 62.7° 2θ values with the (100), (101), (110) crystal planes. Considering SEM–EDX results of Se-NPs, SEM images and EDX signal analysis of selected Se-NPs are presented in Fig. 1C-D. According to the SEM image (Fig. 1C), Se-NPs have a particle size ranging from approximately 28–50 nm and a spherical shape. Additionally, agglomerated NPs attributed to green synthesis are observed to exhibit a layered structure by clustering with each other. Elemental analysis revealed the presence of a selenium signal in addition to calcium, sodium, and oxygen peaks (Fig. 1D). Consequently, it confirmed the presence of 48.5% (by weight) selenium in the sample. Furthermore, calcium (18% by weight) and oxygen (28.7% by weight) signals were detected in the analysis.

The effect of Se-NP applications on morphology development

The results of the three-way ANOVA revealed the effects of Se-NP treatments on the morphological, physiological, and biochemical characteristics of grapevine saplings. The analysis considered the primary factors of different rootstock/scion combinations, irrigation regimes, and NP concentrations, as well as the interactions between these factors (Supplementary Material Table 1). The highest shoot length values were obtained from 1103 P/CS treated with 10 ppm Se-NP under well-irrigated conditions (42.95 cm), followed by 5 BB/CS under the same conditions (41.30 cm) (Fig. 2A, Supplementary Material Table 2). The lowest averages were recorded from the control of 5 BB/CS (15.70 cm) under drought conditions, the control (16.64 cm) and 100 ppm (16.32 cm) treatments of 41 B/CS, and the control (17.28 cm), 10 ppm (17.31 cm), and 100 ppm (16.92 cm) treatments of 1103 P/CS. Drought stress caused significant reductions in shoot length values for all three rootstock/scion combinations compared to well-irrigated conditions ($p < 0.001$). In the context of drought stress, shoot fresh weight values significantly decreased (6.57 g, $p < 0.001$) compared to well-irrigated conditions (9.75 g). The highest values were obtained from the 10 ppm Se-NP treatment (9.35 g), while the lowest averages were recorded in the control group (7.29 g). Among the rootstock/scion combinations, the highest averages were obtained from 5 BB/CS (8.27 g). According to the interaction between irrigation regime and rootstock/scion combination, the highest values were obtained from 1103 P/CS under well-irrigated conditions (10.33 g), while the lowest averages were from 1103 P/CS under drought conditions (6.33 g). Regarding the interaction between rootstock/scion combination and NP concentration, the maximum values were obtained at 10 ppm Se-NP concentration in all three

(See figure on next page.)

Fig. 1 **A** UV–Vis absorption spectrum of CSe_2 NPs; **B** XRD analysis of CSe_2 NPs synthesized using grapevine extract; **C** SEM images of CSe_2 NPs synthesized using grapevine extract; **D** EDX images of CSe-NPs synthesized using grapevine extract

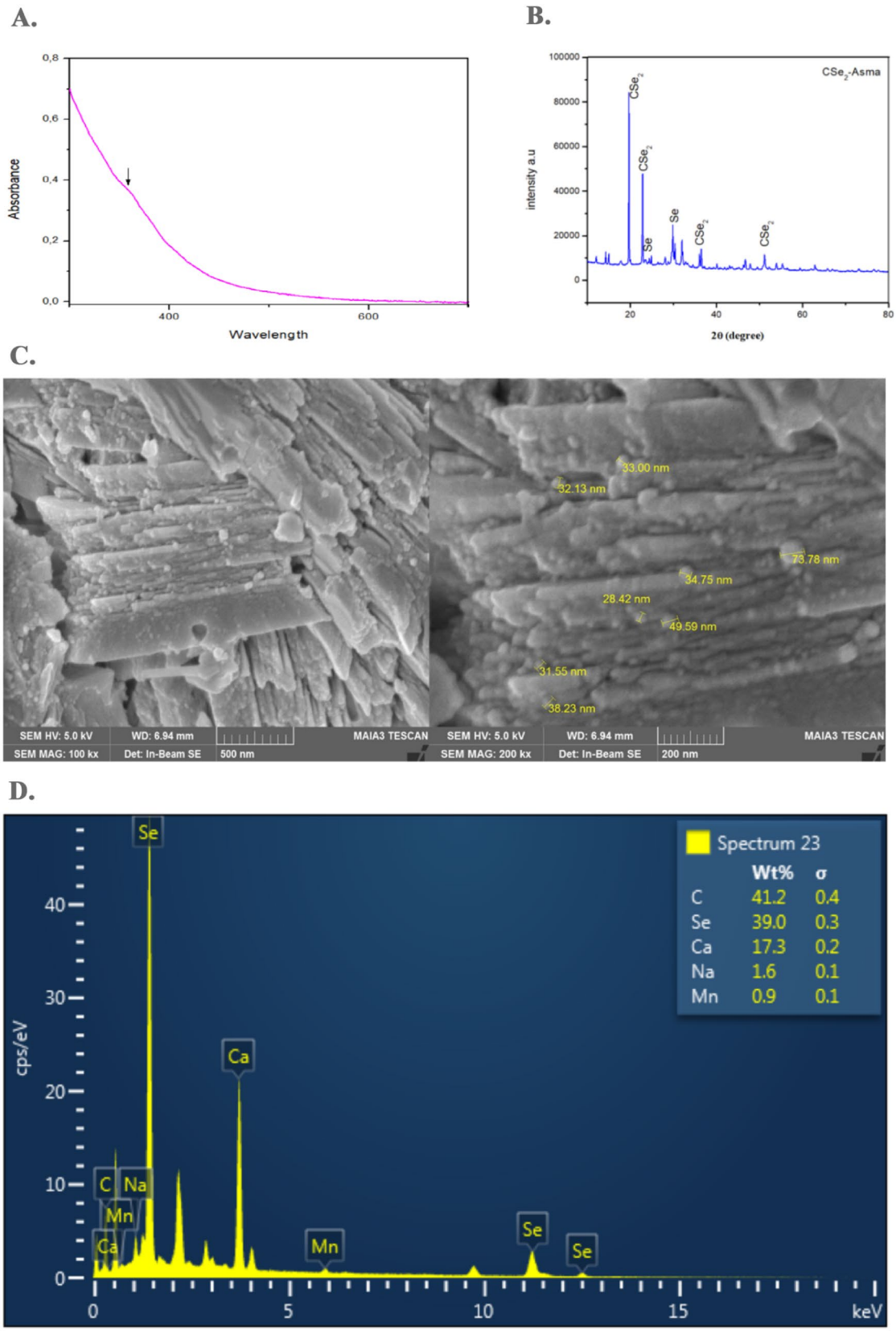


Fig. 1 (See legend on previous page.)

rootstock/scion combinations (5 BB/CS: 9.32 g, 41 B/CS: 9.20 g, and 1103 P/CS: 9.53 g). The highest values according to the interaction between irrigation regime and NP concentration were obtained from the 10 ppm Se-NP treatment under well-irrigated conditions (11.45 g), while the lowest averages were recorded in the control, 1 ppm, and 100 ppm Se-NP treatments under drought conditions (6.07, 6.44, and 6.52 g, respectively) (Fig. 2B, Supplementary Material Table 6). Shoot dry weight values significantly decreased under drought stress (1.86 g, $p < 0.001$) compared to well-irrigated conditions (3.24 g). The highest values were obtained from the 10 ppm Se-NP treatment (3.10 g), while the lowest averages were recorded in the control group (2.22 g). Among the rootstock/scion combinations, the highest averages were obtained from 1103 P/CS (2.73 g). According to the interaction between irrigation regime and rootstock/scion combination, the highest values were obtained from 1103 P/CS under well-irrigated conditions (3.64 g), while all three rootstocks had the lowest average values under drought conditions. Regarding the interaction between rootstock/scion combination and Se-NP concentration, the highest values were obtained from the 10 ppm Se-NP treatment of 1103 P/CS (3.42 g), while the lowest values were obtained from the control of 5 BB/CS (2.05 g) and the control and 100 ppm Se-NP treatments of 41 B/CS (2.12 and 2.18 g, respectively). The highest values according to the interaction between irrigation regime and NP concentration were obtained from the 10 ppm Se-NP treatment under well-irrigated conditions (4.11 g), while the lowest averages were recorded in the control under drought conditions (1.64 g) (Fig. 2C, Supplementary Material Table 7).

As shown in Fig. 2D, shoot dry matter ratio significantly decreased under drought stress (28.39%, $p < 0.001$) compared to well-irrigated conditions (33.08%) (Supplementary Material Table 11). The average number of leaves significantly decreased under drought stress (7.97 pieces, $p < 0.001$) compared to well-irrigated conditions (10.06 pieces). The highest values were obtained from the 10 ppm Se-NP treatment (9.91 pieces), while the lowest averages were recorded in the control group (8.31 pieces). Among the rootstock/scion combinations, the highest averages were obtained from 5 BB/CS (9.33 pieces). According to the interaction between irrigation regime and rootstock/scion combination, the highest values were obtained from 5 BB/CS (10.25 pieces) and 1103 P/CS (10.08 pieces) under well-irrigated conditions, while the lowest averages were obtained from 41 B/CS (7.90 pieces) and 1103 P/CS (7.61 pieces) under drought conditions. Regarding the interaction between rootstock/scion combination and Se-NP concentration, the maximum values were obtained from 5 BB/CS at 100 ppm (9.97 pieces), 41 B/CS at 1 ppm (9.42 pieces) and 10 ppm (9.56 pieces), and 1103 P/CS at 10 ppm (10.35 pieces) Se-NP concentrations (Fig. 2E, Supplementary Material Table 6). Drought stress caused significant reductions in leaf area values for all three rootstock/scion combinations compared to well-irrigated plants ($p = 0.001$). The highest averages in terms of leaf area were obtained from the 10 ppm Se-NP treatment under well-irrigated conditions for all three rootstocks (1103 P/CS: 76.64 cm^2; 5 BB/CS: 75.43 cm^2; 41 B/CS: 74.09 cm^2). The lowest values were obtained from the drought control treatment of 5 BB/CS (47.13 cm^2) and the 100 ppm Se-NP treatment of 41 B/CS under drought conditions (49.08 cm^2) (Fig. 2F, Supplementary Material Table 2). Root length values significantly decreased under drought stress (23.42 cm, $p < 0.001$) compared to well-irrigated conditions (27.59 cm). The highest values were obtained from the 10 ppm Se-NP treatment (27.99 cm), while the lowest averages were recorded in the control group (23.61 cm). Among the rootstock/scion combinations, the highest averages were obtained from 5 BB/CS (26.18 cm). According to the interaction between irrigation regime and rootstock/scion combination, the highest values were obtained from all three rootstock/scion combinations under well-irrigated conditions (5 BB/CS: 27.90 cm, 41 B/CS: 27.15 cm, and 1103 P/CS: 27.71 cm). The lowest averages were recorded at 41 B/CS (23.30 cm) and 1103 P/CS (22.49 cm) under drought conditions. Regarding the interaction between rootstock/scion combination and NP concentration, the maximum values were obtained from 5 BB/CS at 10 ppm (28.07 cm) and 100 ppm (27.27 cm) Se-NP concentrations, and from 1103 P/CS at 10 ppm (28.37 cm). The highest values according to the interaction between irrigation regime and NP concentration were obtained from the 10 ppm Se-NP treatment under well-irrigated conditions (30.79 cm), while the lowest averages were recorded in the control and 100 ppm Se-NP treatments under drought conditions (21.66 and 22.76 cm, respectively) (Fig. 3A, Supplementary Material Table 7).

Root fresh weight significantly decreased under drought conditions for all three rootstock/scion combinations ($p < 0.001$). The highest values were obtained from the 10 ppm Se-NP treatment of 1103 P/CS under well-irrigated conditions (6.92 g), while the lowest averages were obtained from the control treatment of 5 BB/CS under drought conditions (2.15 g) (Fig. 3B, Supplementary Material Table 2). Root dry weight values significantly decreased under drought stress (1.51 g, $p < 0.001$) compared to well-irrigated conditions (2.89 g). The highest values were obtained from the 10 ppm Se-NP treatment (2.87 g), while the lowest averages were recorded in the control group (1.86 g). Among the rootstock/scion combinations, the highest averages were obtained from 1103 P/CS (2.32 g). According to the interaction between

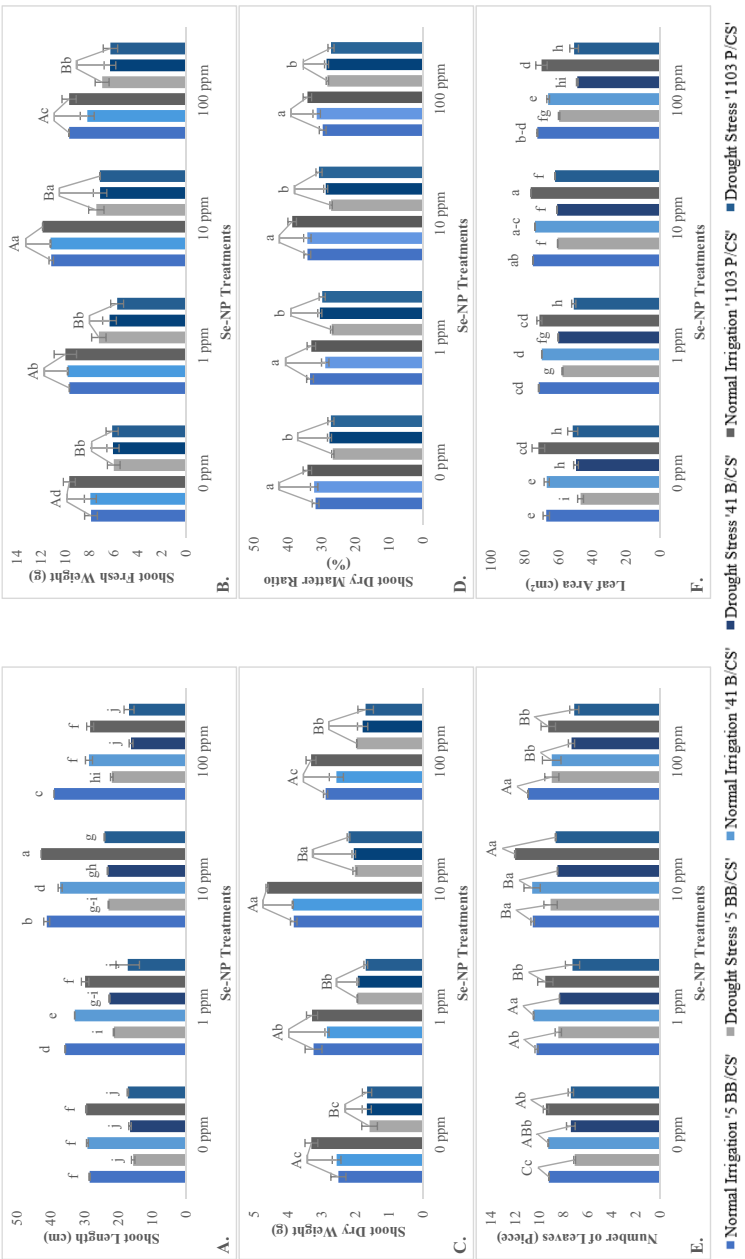


Fig. 2 Effect of Se-NPs against drought stress on shoot and leaf characteristics of grapevine saplings. *Different letters indicate significant differences based on Duncan's post hoc analysis at $p \leq 0.05$. Data are mean values ± SE

irrigation regime and rootstock/scion combination, the highest values were obtained from 1103 P/CS under well-irrigated conditions (3.10 g), while the lowest averages were recorded from 41 B/CS under drought conditions (1.40 g). Regarding the interaction between rootstock/scion combination and NP concentration, the highest values were obtained from the 10 ppm Se-NP treatment of 1103 P/CS (3.29 g), while the lowest values were obtained from the 100 ppm Se-NP treatment of 41 B/CS (1.76 g). The highest values according to the interaction between irrigation regime and Se-NP concentration were obtained from the 10 ppm Se-NP treatment under well-irrigated conditions (3.90 g), while the lowest averages were recorded in the control and 100 ppm Se-NP treatments under drought conditions (1.28 and 1.37 g, respectively) (Fig. 3C, Supplementary Material Table 8). Root dry matter ratio did not show a significant change between drought stress and well-irrigated conditions ($p = 0.218$). The highest values were obtained from the 10 ppm Se-NP treatment (64.01%), while the lowest averages were recorded in the control group (56.88%). Among the rootstock/scion combinations, the highest averages were obtained from 5 BB/CS (65.02%). According to the interaction between irrigation regime and rootstock/scion combination, the highest values were obtained from 5 BB/CS (66.46%) and 41 B/CS (64.01%) under well-irrigated conditions and from 5 BB/CS (63.58%) and 1103 P/CS (63.77%) under drought stress, while the lowest averages were recorded from 1103 P/CS under well-irrigated conditions (52.34%) and from 41 B/CS under drought conditions (51.30%). Regarding the interaction between rootstock/scion combination and Se-NP concentration, the maximum values were obtained from 1 ppm in 5 BB/CS (70.82%) and 10 ppm Se-NP concentration in 1103 P/CS (66.86%) (Fig. 3D, Supplementary Material Table 8).

The effect of Se-NP applications on physiological parameters

Drought stress significantly reduced the relative water content (RWC) of leaves in all three rootstock/scion combinations ($p < 0.001$) (Supplementary Material Table 1). The highest RWC values were obtained from the 10 ppm Se-NP treatment of 1103 P/CS under well-irrigated conditions (84.92%), while the lowest values were recorded from the control treatment of 5 BB/CS under drought conditions (41.61%) (Fig. 3E, Supplementary Material Table 3). Stomatal conductance also decreased significantly under drought stress compared to well-irrigated conditions across all three rootstock/scion combinations ($p < 0.001$). The highest values were recorded from the 10 ppm Se-NP treatment of 1103 P/CS under well-irrigated conditions (130.80 mmol m^{-2} s^{-1}), whereas the lowest values were observed in the control treatments under drought conditions (5 BB/CS: 81.45 mmol m^{-2} s^{-1}; 41 B/CS: 81.95 mmol m^{-2} s^{-1}; 1103 P/CS: 80.20 mmol m^{-2} s^{-1}) (Fig. 3F, Supplementary Material Table 3). The SPAD index values significantly decreased under drought stress compared to well-irrigated conditions (32.92 SPAD compared to 38.30 SPAD, $p < 0.001$). The highest SPAD values were obtained from the 10 ppm Se-NP treatment (39.19 SPAD), while the lowest values were observed in the control group (33.73 SPAD). Among the rootstock/scion combinations, the highest values were obtained from 5 BB/CS (37.70 SPAD). According to the interaction between irrigation regime and rootstock/scion combination, the highest values were recorded from 5 BB/CS under well-irrigated conditions (40.43 SPAD), while the lowest values were obtained from 1103 P/CS under drought conditions (31.25 SPAD). Regarding the interaction between rootstock/scion combination and Se-NP concentration, the highest values were recorded from 5 BB/CS and 1103 P/CS at 10 ppm Se-NP concentration (39.86 and 39.30 SPAD, respectively), while the lowest values were obtained from 41 B/CS and 1103 P/CS at 100 ppm Se-NP concentration (31.19 and 30.80 SPAD, respectively). The interaction between irrigation regime and NP concentration showed the highest values from the 10 ppm Se-NP treatment under well-irrigated conditions (42.96 SPAD), whereas the lowest values were observed in the control and 100 ppm Se-NP treatments under drought conditions (31.52 and 31.34 SPAD, respectively) (Fig. 4A, Supplementary Material Table 9).

Leaf surface temperature significantly increased under drought stress compared to well-irrigated conditions (26.78 °C vs. 25.31 °C, $p < 0.001$). The highest temperatures among the concentrations were observed in the 100 ppm Se-NP treatment (26.28 °C), while the lowest averages were recorded in the control, 1 ppm, and 10 ppm Se-NP treatments. Among the rootstock/scion combinations, the lowest averages were obtained from 1103 P/CS (25.95 °C). Considering the interaction between irrigation regime and Se-NP concentration, the lowest value was in the well-irrigated control treatment (24.80 °C), while the highest averages were observed in the drought-stressed control and 100 ppm Se-NP treatments (27.13 °C and 27.06 °C, respectively) (Fig. 4B, Supplementary Material Table 9). Drought stress significantly increased the drought indices of all three rootstock/scion combinations ($p < 0.001$). The lowest drought index values were obtained from the well-irrigated treatments (0.00%); the highest averages were obtained from the drought-stressed control treatments for each rootstock (5 BB/CS: 56.78%; 41 B/CS: 51.59%; 1103 P/CS: 47.18%). However, the most effective treatments in reducing the drought index values under drought conditions were the 10 ppm

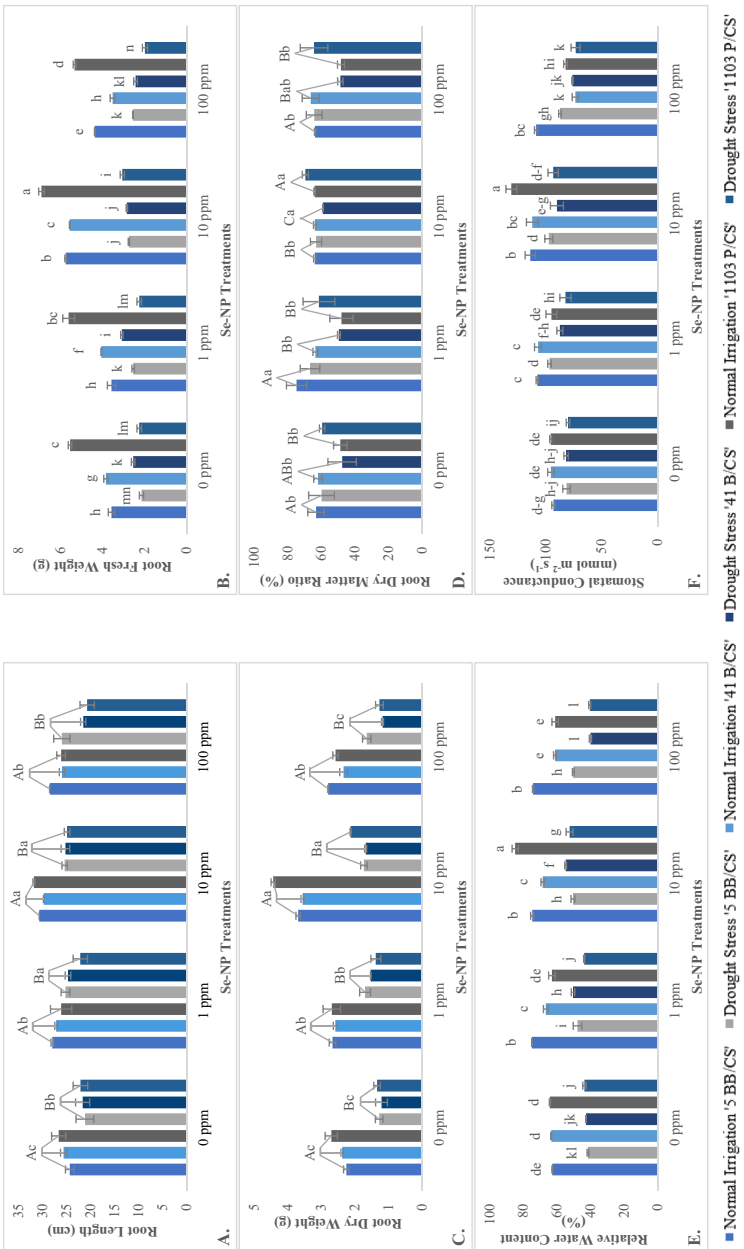


Fig. 3 Effect of Se-NPs on root properties, relative water content and stomatal conductance of grapevine saplings against drought stress. *Different letters indicate significant differences based on Duncan's post hoc analysis at $p \leq 0.05$. Data are mean values ± SE

Se-NP groups (5 BB/CS: 33.62%; 41 B/CS: 35.65%; 1103 P/CS: 37.12%) (Fig. 4C, Supplementary Material Table 3). Drought stress also caused a significant increase in the electrolyte leakage (EL) values of all three rootstock/scion combinations ($p < 0.001$). The lowest EL values for each rootstock were obtained from the well-irrigated control (5 BB/CS: 5.36%; 41 B/CS: 5.34%; and 1103 P/CS: 5.16%) and 1 ppm Se-NP treatments (5 BB/CS: 5.57%; 41 B/CS: 5.51%; and 1103 P/CS: 5.42%). The highest averages were obtained from 41 B/CS and 1103 P/CS rootstocks treated with 100 ppm Se-NP under drought conditions (27.03% and 26.19%, respectively). The most effective treatments in reducing EL under drought conditions were the 10 ppm Se-NP treatments for all three rootstocks (5 BB/CS: 16.24%; 41 B/CS: 15.92%; and 1103 P/CS: 15.49%) (Fig. 4D, Supplementary Material Table 4).

The effect of Se-NP applications on biochemical parameters

Under drought conditions, H_2O_2 production showed a significant increase in all three rootstock/scion combinations, paralleling the trend observed in EL ($p = 0.003$). The highest averages were obtained from the control treatments under drought stress for all three rootstocks (5 BB/CS: 31.31 µmol g^{-1}; 41 B/CS: 30.85 µmol g^{-1}; and 1103 P/CS: 30.30 µmol g^{-1}). The lowest averages were recorded from the control treatments under well-irrigated conditions for all three rootstocks (5 BB/CS: 10.82 µmol g^{-1}; 41 B/CS: 10.46 µmol g^{-1}; and 1103 P/CS: 9.55 µmol g^{-1}) and from the 1 ppm Se-NP treatment of well-irrigated 1103 P/CS (9.97 µmol g^{-1}) (Fig. 4E, Supplementary Material Table 4). Malondialdehyde (MDA) levels significantly increased under drought stress compared to well-irrigated conditions (6.71 nmol g^{-1} vs. 2.20 nmol g^{-1}, $p < 0.001$). The highest values were observed in the 100 ppm Se-NP treatment (5.01 nmol g^{-1}), while the lowest averages were found in the 1 and 10 ppm Se-NP treatments (4.09 and 3.99 nmol g^{-1}, respectively). The highest values among the rootstock/scion combinations and Se-NP concentrations were obtained from the control treatment of 5 BB/CS (4.97 nmol g^{-1}) and from the 100 ppm Se-NP treatments of all three rootstocks (5 BB/CS: 4.97 nmol g^{-1}; 41 B/CS: 5.28 nmol g^{-1}; 1103 P/CS: 4.78 nmol g^{-1}). The lowest values were found in the well-irrigated control treatment (1.51 nmol g^{-1}), while the highest averages were recorded in the drought-stressed control treatment (7.96 nmol g^{-1}) (Fig. 4F, Supplementary Material Table 10). Proline content significantly increased under drought stress compared to well-irrigated conditions (0.89 µmol g^{-1} vs. 0.49 µmol g^{-1}, $p < 0.001$). The highest values were observed in the 100 ppm Se-NP treatment (0.76 µmol g^{-1}), while the lowest averages were found in the 1 and 10 ppm Se-NP treatments (0.65 µmol g^{-1}). The highest averages among the rootstock/scion combinations were obtained from 5 BB/CS and 41 B/CS (0.70 and 0.71 µmol g^{-1}, respectively), whereas the lowest averages were from 1103 P/CS (0.65 µmol g^{-1}). The highest values considering the interaction between irrigation regime and rootstock/scion combinations were obtained from 5 BB/CS and 41 B/CS under drought conditions (0.94 and 0.89 µmol g^{-1}, respectively), while the lowest averages were recorded from well-irrigated 5 BB/CS and 1103 P/CS (0.47 and 0.46 µmol g^{-1}, respectively). The lowest values considering the interaction between irrigation regime and NP concentration were found in the well-irrigated control treatment (0.36 µmol g^{-1}), while the highest averages were recorded in the drought-stressed control treatment (1.04 µmol g^{-1}) (Fig. 5A, Supplementary Material Table 10).

Total phenolic content significantly increased under drought stress in all three rootstock/scion combinations ($p < 0.001$). The highest values were obtained from the drought-stressed control treatment of 5 BB/CS (20.69 mg g^{-1}), while the lowest values were recorded from the well-irrigated control treatments of all three rootstocks (5 BB/CS: 3.21 mg g^{-1}; 41 B/CS: 3.63 mg g^{-1}; and 1103 P/CS: 4.05 mg g^{-1}) and from the 1 ppm Se-NP treatments (5 BB/CS: 4.38 mg g^{-1}; 41 B/CS: 4.14 mg g^{-1}; and 1103 P/CS: 4.41 mg g^{-1}). Additionally, Se-NP treatments effectively reduced total phenolic content under drought stress, with the lowest averages obtained from the 10 ppm Se-NP treatments of all three rootstocks (5 BB/CS: 14.07 mg g^{-1}; 41 B/CS: 13.09 mg g^{-1}; and 1103 P/CS: 13.73 mg g^{-1}) (Fig. 5B, Supplementary Material Table 4). Total soluble protein content significantly decreased under drought stress compared to well-irrigated conditions (0.77 mg vs. 3.28 mg, $p < 0.001$). The highest values among the concentrations were observed in the 10 ppm Se-NP treatment (2.35 mg), while the lowest averages were recorded in the control and 100 ppm Se-NP treatments (1.77 and 1.83 mg, respectively). The highest values considering the interaction between irrigation regime and rootstock/scion combinations were obtained from well-irrigated 1103 P/CS (3.47 mg), while the lowest averages were recorded from drought-stressed 1103 P/CS (0.71 mg). The highest values considering the interaction between rootstock/scion combinations and NP concentrations were obtained from the 10 ppm Se-NP treatments of all three rootstocks (5 BB/CS: 2.45 mg; 41 B/CS: 2.21 mg; 1103 P/CS: 2.40 mg) and from the 1 ppm Se-NP treatment of 1103 P/CS (2.18 mg), while the lowest values were recorded from the 100 ppm Se-NP treatment of 5 BB/CS and the control treatment of 41 B/CS (1.59 and 1.75 mg, respectively). The highest values considering the interaction between irrigation regime

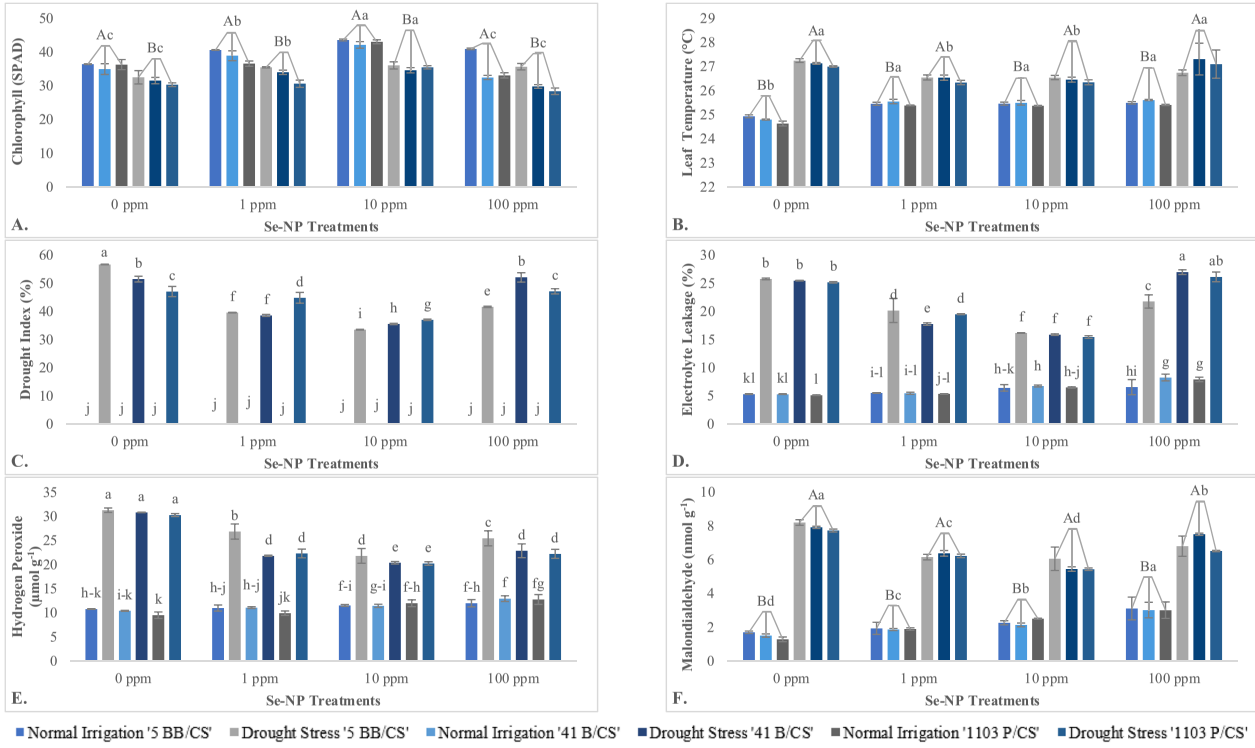


Fig. 4 Effect of Se-NPs on chlorophyll content and oxidative stress parameters of grapevine saplings against drought stress. *Different letters indicate significant differences based on Duncan's post hoc analysis at $p \leq 0.05$. Data are mean values ± SE

and Se-NP concentrations were obtained from the well-irrigated 10 ppm Se-NP treatment (3.77 mg), while the lowest averages were recorded from the drought-stressed control treatment (0.59 mg) (Fig. 5C, Supplementary Material Table 11). Drought stress caused significant increases in the activities of SOD, CAT, and APX enzymes in all three rootstock/scion combinations (SOD: $p=0.003$; CAT: $p=0.001$; APX: $p=0.002$). The highest SOD activity was obtained from the drought-stressed control treatment of 5 BB/CS (81.10 U mg^{-1}), followed by the control treatments of 41 B/CS (78.19 U mg^{-1}) and 1103 P/CS (74.30 U mg^{-1}). The lowest SOD activity was observed in the well-irrigated control groups of 5 BB/CS, 41 B/CS, and 1103 P/CS (21.96 U mg^{-1}; 21.34 U mg^{-1}; and 20.63 U mg^{-1}, respectively) (Fig. 5D, Supplementary Material Table 5). The highest CAT activity was obtained from the drought-stressed control treatment of 5 BB/CS (0.36 U mg^{-1}), followed by the 100 ppm Se-NP treatment of 5 BB/CS (0.32 U mg^{-1}). The lowest CAT values were recorded in the well-irrigated control treatments of all three rootstocks (0.02 U mg^{-1}). However, under drought stress, the 10 ppm Se-NP treatment significantly reduced CAT activity compared to drought-stressed controls for all three rootstocks (5 BB/CS: 0.23 U mg^{-1}; 41 B/CS: 0.17 U mg^{-1}; 1103 P/CS: 0.12 U mg^{-1}) (Fig. 5E, Supplementary Material Table 5). APX activity peaked at 9.10 U mg^{-1} in the drought-stressed control treatment of 5 BB/CS, followed by the control treatments of 41 B/CS (8.38 U mg^{-1}) and 1103 P/CS (8.01 U mg^{-1}). The lowest averages were observed in all well-irrigated treatments with and without Se-NP applications (Fig. 5F, Supplementary Material Table 5).

General evaluation

Pearson correlation analysis revealed strong positive correlations among plant growth parameters, except for root dry matter ratio. The strongest positive correlations among plant growth parameters were observed between shoot dry weight and shoot fresh weight (0.98), root dry weight and shoot dry weight (0.98) and shoot length and leaf number (0.97). Among physiological parameters, the strongest positive correlations were between membrane damage index and drought index (0.98), membrane damage index and leaf temperature (0.96), and drought index and leaf temperature (0.95). The strongest negative correlations among physiological parameters were between membrane damage index and RWC (−0.90), drought index and RWC (−0.91), and leaf temperature and RWC (−0.83). The strongest positive correlations between physiological parameters and plant growth characteristics were found to be between RWC and shoot length (0.98), RWC and leaf number (0.96), and RWC and leaf area (0.95). The strongest negative correlations between physiological parameters and plant growth characteristics were identified as membrane damage index and leaf area (−0.95), drought index and leaf area (−0.94), and drought index and shoot length (−0.89). Among biochemical parameters, the strongest positive correlations were observed between total phenolic content and lipid peroxidation (0.98), APX and hydrogen peroxide content (0.98), and SOD and APX (0.97). The strongest negative correlations among biochemical parameters were found between soluble protein content and lipid peroxidation (−0.94), soluble protein content and hydrogen peroxide content (−0.91), and soluble protein content and total phenolic content (−0.91). The strongest positive correlations between biochemical parameters and plant growth characteristics were identified as soluble protein content and shoot fresh weight (0.92), soluble protein content and shoot dry weight (0.92), and soluble protein content and leaf area (0.91). The strongest negative correlations between biochemical parameters and plant growth characteristics were found to be APX and leaf area (−0.93), lipid peroxidation and leaf area (−0.92), and hydrogen peroxide content and leaf area (−0.90). The strongest positive correlations between biochemical and physiological parameters were observed between lipid peroxidation and membrane damage index (0.98), lipid peroxidation and drought index (0.98), and lipid peroxidation and leaf temperature (0.97). The strongest negative correlations between biochemical and physiological parameters were identified as soluble protein content and drought index (-0.96), soluble protein content and membrane damage index (−0.92), and soluble protein content and leaf temperature (−0.88) (Fig. 6).

Experimental data were subjected to PCA for a general evaluation of agronomic, physiological, and biochemical parameters. The first three components had eigenvalues > 1.0. Among these, the first two principal components explained 89.72% of the variability of the original data. The high proportion of variance explained by these components indicates that the evaluated variables can be strongly explained by the principal component analysis. Therefore, based on the scores of the first two components, the experimental groups were distributed within a PCA graph (Fig. 7). The well-irrigated group of applications was in the negative loading value of the first principal component (PC1), which accounted for 81.33% of the total variation. These applications were represented by higher averages in growth parameters and some physiological characteristics. The applications closest to the well-irrigated controls were 1103P/CS-WI-1 and 1103P/CS-WI-100, which had the highest values in total soluble protein content. However, 1103P/CS-WI-10, 5BB/CS-WI-10, and 41B/CS-WI-10 applications showed higher performance in plant growth characteristics,

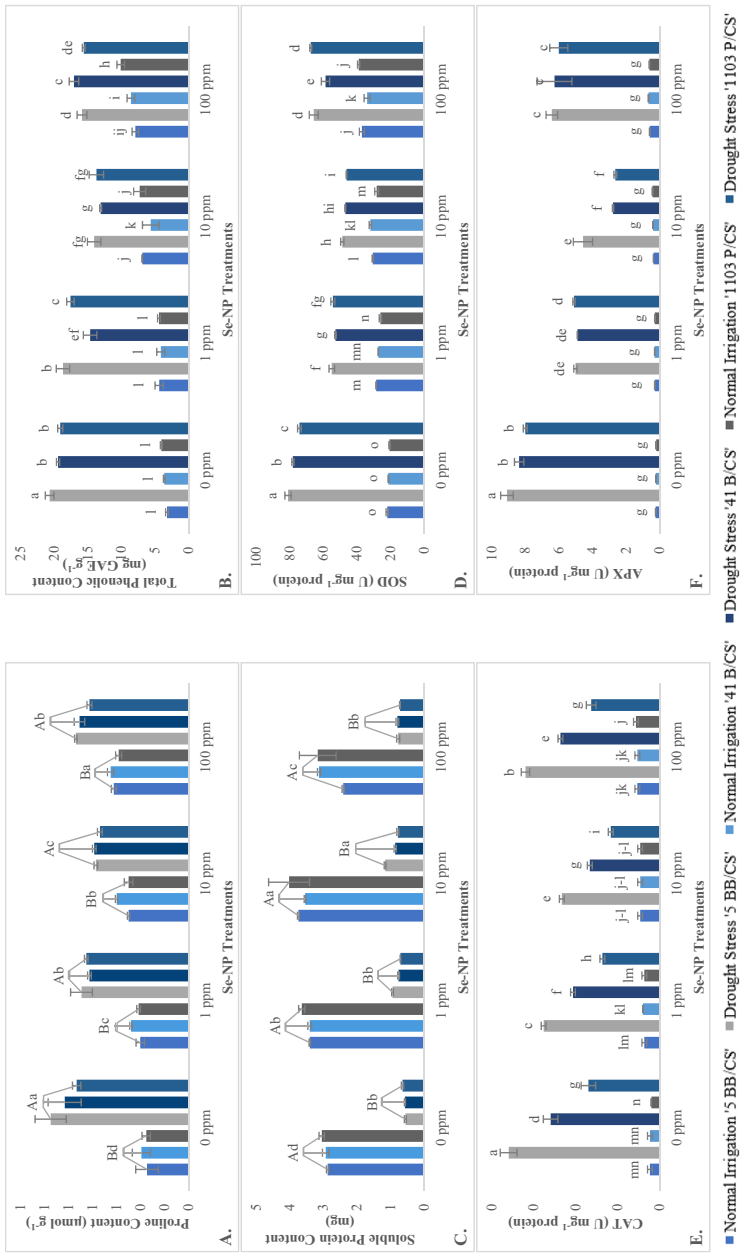


Fig. 5 Effect of Se-NPs on antioxidant enzyme activities, proline, total soluble protein and total phenolic content of grapevine saplings against drought stress. *Different letters indicate significant differences based on Duncan's post hoc analysis at $p \leq 0.05$. Data are mean values ± SE

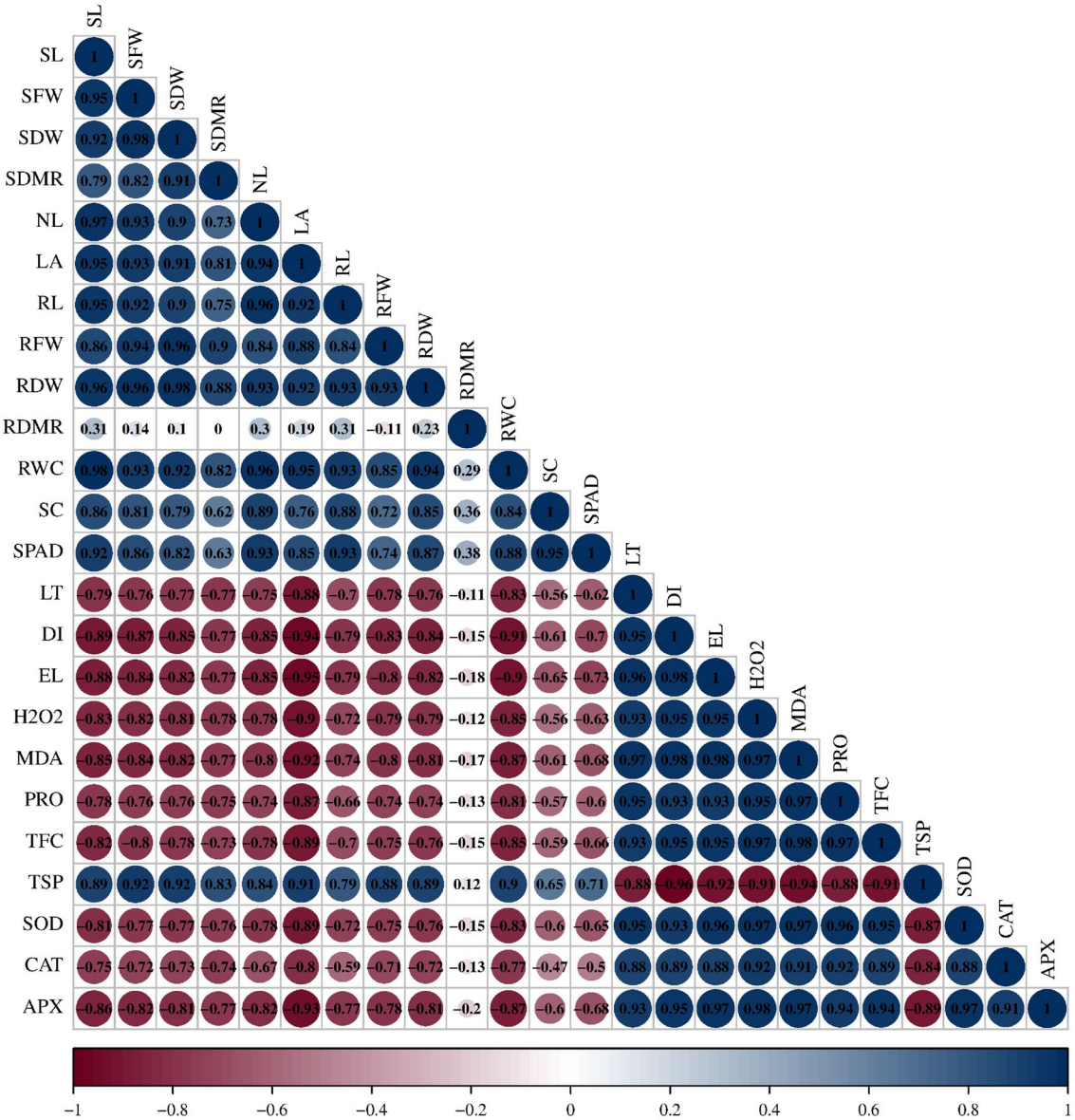


Fig. 6 Correlation analysis of different irrigation regimes, Se-NP doses and rootstock/scion combinations on the studied traits in grapevine saplings. In the correlation table, *NL* number of leaves, *LA* leaf area, *SL* shoot length, *SFW* shoot fresh weight, *SDW* shoot dry weight, *SDMR* shoot dry matter ratio, *RL* root length, *RFW* root fresh weight, *RDW* root dry weight, *RDMR* root dry matter ratio, *SPAD* chlorophyll content, *RWC* relative water content, *SC* stomatal conductance, *DI* drought index, *LT* leaf temperature, *EL* electrolyte leakage, H_2O_2 hydrogen peroxide, *MDA* malondialdehyde, *PRO* proline content, *TPC* total phenolic content, *TSP* soluble protein content, *SOD* superoxide dismutase, *CAT* catalase and *APX* ascorbate peroxidase enzyme activity

SPAD index, RWC, and stomatal conductance parameters compared to the irrigated control applications. All applications under drought stress were in the positive loading value of PC1. The drought control applications were represented by higher averages in oxidative stress parameters and in antioxidant properties. Within the drought group, the applications 1103P/CS-DS-100, 41B/CS-DS-100, and 1103P/CS-DS-1 showed the lowest averages in these characteristics. However, the applications 1103P/CS-DS-10, 5BB/CS-DS-10, and 41B/CS-DS-10 had lower oxidative stress parameters and antioxidant properties, but higher averages in plant growth parameters, SPAD index, RWC, and stomatal conductance. The second principal component (PC2), accounting for 8.39%

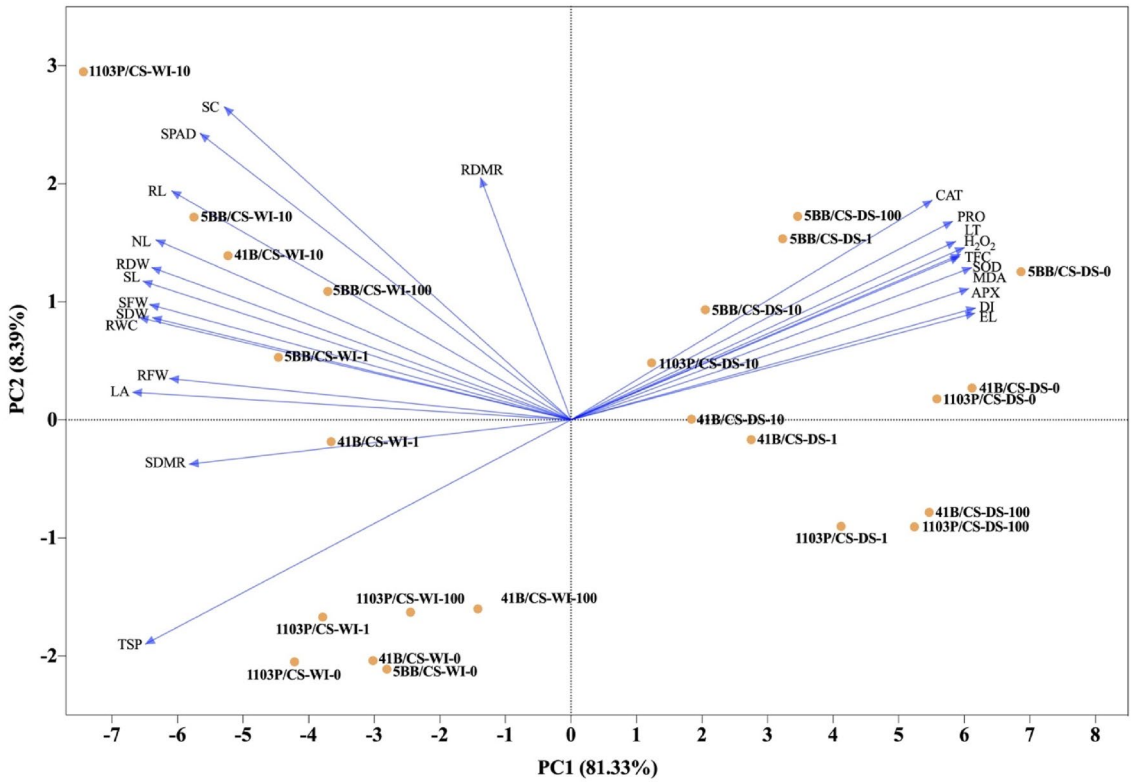


Fig. 7 Principal component analysis (PCA) to determine the effects of different irrigation regimes, Se-NP doses and rootstock/scion combinations on the studied traits in grapevine saplings. In PCA, *NL* number of leaves, *LA* leaf area, *SL* shoot length, *SFW* shoot fresh weight, *SDW* shoot dry weight, *SDMR* shoot dry matter ratio, *RL* root length, *RFW* root fresh weight, *RDW* root dry weight, *RDMR* root dry matter ratio, *SPAD* chlorophyll content, *RWC* relative water content, *SC* stomatal conductance, *DI* drought index, *LT* leaf temperature, *EL* electrolyte leakage, H_2O_2 hydrogen peroxide, *MDA* malondialdehyde, *PRO* proline content, *TPC* total phenolic content, *TSP* soluble protein content, *SOD* superoxide dismutase, *CAT* catalase and *APX* ascorbate peroxidase enzyme activity, *5BB/CS* 5 BB/CS rootstock/scion combination, *41B/CS* 41 B/CS rootstock/scion combination, *1103P/CS* 1103 P/CS rootstock/scion combination, *WI* well-irrigated group, *DS* drought stress treated group, *0* control treatment without nanoparticles, *1* 1 ppm nanoparticles treatment, *10* 10 ppm nanoparticles treatment and *100* 100 ppm nanoparticles treatment

of the total variation, indicated that the 41B/CS-WI-100 application had the lowest performance among the well-irrigated applications, located in the negative loading value of PC2. A hierarchical clustering heat map was generated to visualize, clarify, and relate the findings with experimental groups (Fig. 8). According to the clustering in the heat map, the examined traits were divided into two main clusters. Leaf temperature, drought and membrane damage index, antioxidant enzyme activities, lipid peroxidation, hydrogen peroxide, proline, and phenolic content were grouped in the first main cluster, while plant growth parameters, soluble protein content, stomatal conductance, and SPAD index were grouped in the second main cluster. The heat map generally divided Se-NP applications into two main clusters, representing well-irrigated and drought stress groups. The first main cluster included well-irrigated applications represented by lower averages in stress parameters, antioxidant enzyme activities, proline, and total phenolic content, but higher averages in plant growth parameters, soluble protein content, RWC, stomatal conductance, and SPAD index. In the first main cluster, the 41B/CS-WI-100 application showed a distinct separation from other well-irrigated samples due to higher oxidative stress parameters and lower growth characteristics, forming a separate subgroup. In the second main cluster, drought applications were represented by lower averages in plant growth parameters, soluble protein content, RWC, stomatal conductance, and SPAD index, but higher averages in stress parameters such as leaf temperature, drought and membrane damage index, antioxidant enzyme activities, lipid peroxidation, hydrogen peroxide, proline, and phenolic content. Within the second main cluster, the 1103P/CS-DS-10 application formed the first subcluster with lower oxidative stress parameters and higher growth characteristics and improved physiological performance.

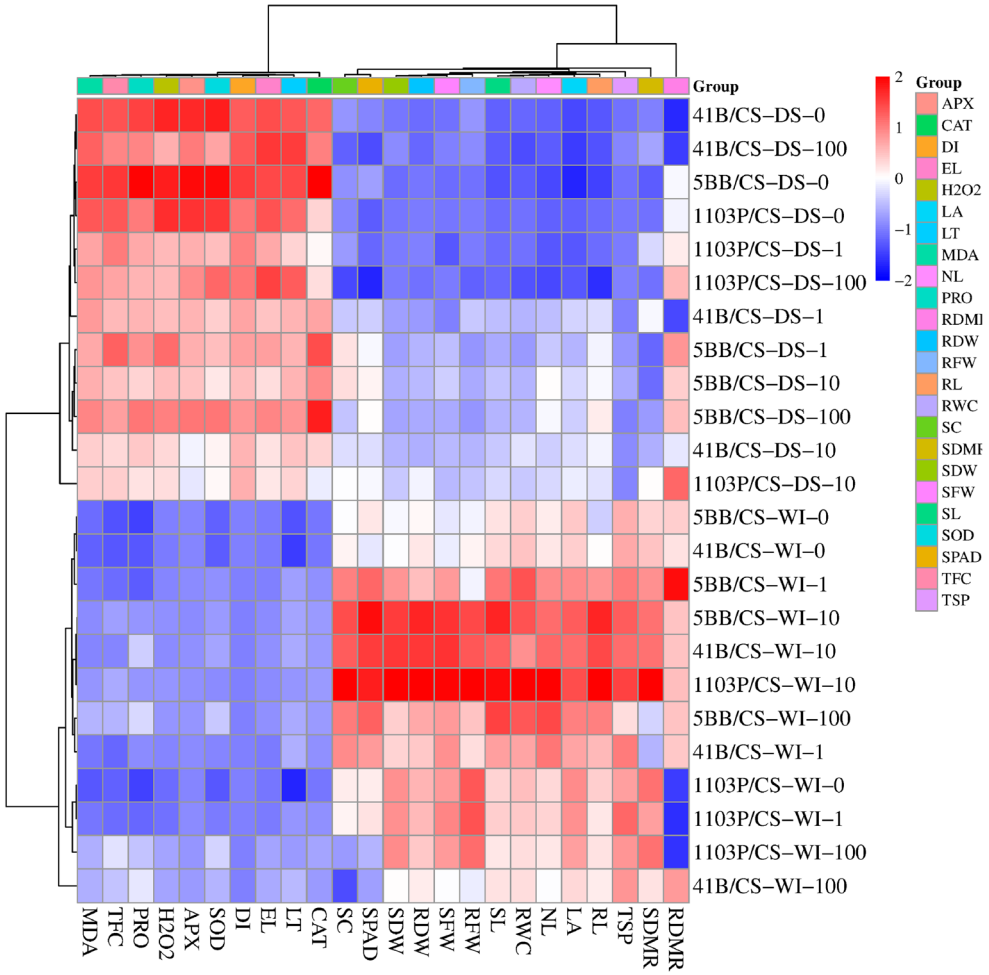


Fig. 8 Hierarchical clustering heatmap for the effects of different irrigation regimes, Se-NP doses and rootstock/scion combinations on the studied traits in grapevine saplings. In Heatmap, *NL* number of leaves, *LA* leaf area, *SL* shoot length, *SFW* shoot fresh weight, *SDW* shoot dry weight, *SDMR* shoot dry matter ratio, *RL* root length, *RFW* root fresh weight, *RDW* root dry weight, *RDMR* root dry matter ratio, *SPAD* chlorophyll content, *RWC* relative water content, *SC* stomatal conductance, *DI* drought index, *LT* leaf temperature, *EL* electrolyte leakage, H_2O_2 hydrogen peroxide, *MDA* malondialdehyde, *PRO* proline content, *TPC* total phenolic content, *TSP* soluble protein content, *SOD* superoxide dismutase, *CAT* catalase and *APX* ascorbate peroxidase enzyme activity, *5BB/CS* 5 BB/CS rootstock/scion combination, *41B/CS* 41 B/CS rootstock/scion combination, *1103P/CS* 1103 P/CS rootstock/scion combination, *WI* well-irrigated group, *DS* drought stress treated group, *0* control treatment without nanoparticles, *1* 1 ppm nanoparticles treatment, *10* 10 ppm nanoparticles treatment and *100* 100 ppm nanoparticles treatment

Discussion

Characterization of nanoparticles

In this study, the visual observation of the color change from green to dark red in the reaction solution is a preliminary indication of the formation of Se-NPs (Fig. 1). This color change is attributed to the surface plasmon resonance (SPR) phenomenon, which arises due to the collective oscillation of free electrons in the nanoparticles when interacting with light. The UV–Vis spectroscopy analysis further confirms the formation of Se-NPs, showing a slight absorption peak around 357 nm. Although the peak is not very sharp, it is consistent with the reported absorption characteristics of Se-NPs in the literature. The broadening of the peak can be attributed to the polydispersity of the nanoparticles, which is a common occurrence in green synthesis methods. The X-ray diffraction (XRD) analysis provides valuable information about the crystalline structure of the synthesized Se-NPs. The sharp peak points observed in the XRD spectrum indicate the formation of well-crystallized Se-NPs with a cubic crystal structure. The observed peaks can be indexed to the (100), (101), and (110) crystal planes of the CSe_2 phase, confirming the successful synthesis of crystalline Se-NPs. The morphological characterization using scanning electron microscopy (SEM) reveals the size and shape of the synthesized Se-NPs. The SEM image shows

spherical nanoparticles with a size range of approximately 28–50 nm. Additionally, the agglomeration of nanoparticles into a layered structure is observed, which is a common phenomenon in green synthesis methods due to the absence of stabilizing agents. The energy-dispersive X-ray (EDX) analysis provided information about the elemental composition of the synthesized nanoparticles. The EDX spectrum confirmed the presence of selenium, contributing to 48.5% by weight of the sample. The presence of calcium (18% by weight) and oxygen (28.7% by weight) signals can be attributed to the use of plant extracts or other natural precursors in the green synthesis process, which often contain these elements.

The effect of Se-NP applications on morphology development

The present study indicated that drought stress significantly reduced various growth parameters, including shoot length, shoot fresh and dry weight, shoot dry matter ratio, number of leaves, leaf area, root length, root fresh and dry weight, across all three rootstock/scion combinations (1103 P/CS, 5 BB/CS, and 41 B/CS). These findings are consistent with previous reports, where drought stress has been shown to adversely affect plant growth and development in different species [44, 45]. The observed decreases in leaf area and number of leaves under drought stress can be attributed to the plant's defense mechanism against water deficit. As water potential decreases during drought conditions, the leaf area is reduced to minimize water loss through transpiration [45]. Additionally, cell growth is dependent on turgor pressure, which is compromised under water-limited conditions, inhibiting cell division and expansion, ultimately leading to reduced shoot and root lengths [46, 47]. Interestingly, the application of Se-NPs, particularly at a concentration of 10 ppm, significantly improved various growth parameters, including leaf area, number of leaves, shoot length, shoot fresh and dry weight, root length, root fresh and dry weight, and root dry matter ratio, under both well-irrigated and drought stress conditions. These results indicate that Se-NPs can mitigate the negative effects of drought stress on sapling growth and development.

The positive effects of Se-NPs on plant growth under stress conditions have been attributed to the enhancement of photosynthetic and antioxidant enzyme activities [48]. During water deficit, reactive oxygen species (ROS) accumulate, and Se-NPs can activate antioxidant defense mechanisms, thereby reducing the impacts of oxidative stress and improving growth properties [49]. These findings are supported by previous studies reporting the beneficial effects of Se on drought tolerance and fresh and dry weight in crops like maize [50]. Furthermore, the study revealed that the rootstock/scion combination and the interaction between rootstock/scion, irrigation regime, and Se-NP concentration significantly influenced various growth parameters. For instance, the highest shoot length values were observed in 1103 P/CS and 5 BB/CS treated with 10 ppm Se-NPs under well-irrigated conditions (Fig. 2A, Supplementary Material Table 2). Similarly, the highest root fresh weight was obtained from the 10 ppm Se-NP treatment of 1103 P/CS under well-irrigated conditions (Fig. 3B, Supplementary Material Table 2). These results suggest that the rootstock/scion combination plays a crucial role in determining the plant's response to Se-NP treatments and drought stress.

The effect of Se-NP applications on physiological parameters

Our results indicated that drought stress significantly reduced the relative water content (RWC) and stomatal conductance while increasing leaf surface temperature, drought index, and electrolyte leakage across all three rootstock/scion combinations (1103 P/CS, 5 BB/CS, and 41 B/CS). The reduction in RWC under drought stress can be attributed to the plant's inability to maintain water balance due to limited water availability in the soil. As drought stress persists, plants tend to close their stomata to minimize water loss through transpiration, leading to a decrease in stomatal conductance [51]. This process is often accompanied by a reduction in CO_2 absorption and chlorophyll degradation, which can be exacerbated by the overexpression of the Rubisco enzyme [51]. The observed increase in leaf surface temperature under drought stress conditions is a consequence of reduced transpirational cooling due to stomatal closure [49]. The drought index and electrolyte leakage, which are indicators of cellular membrane damage, were also elevated under drought stress, reflecting the detrimental effects of water deficit on plant cellular integrity [52]. Interestingly, the application of Se-NPs, particularly at a concentration of 10 ppm, significantly improved RWC, stomatal conductance, and the SPAD index (a measure of chlorophyll content), while reducing leaf surface temperature, drought index, and electrolyte leakage under both well-irrigated and drought stress conditions. These findings are consistent with previous studies demonstrating the positive effects of Se-NPs on various physiological parameters in different plant species under stress conditions [53–55]. The beneficial effects of Se-NPs in mitigating drought stress can be attributed to their ability to enhance antioxidant defense mechanisms and protect plants from oxidative stress induced by water deficit conditions. Se-NPs have been reported to stimulate antioxidant enzyme activities, regulate redox reactions, and support chloroplast function, thereby maintaining chlorophyll concentration

and photosynthetic efficiency [49, 56, 57]. Furthermore, Se-NPs can contribute to osmotic adjustment and water homeostasis in plants, allowing them to maintain better hydration and tissue health under drought stress [58]. This mechanism can explain the observed improvements in RWC, stomatal conductance, and reductions in drought index and electrolyte leakage in Se-NP-treated plants under water-limited conditions. It is noteworthy that the rootstock/scion combination and the interaction between rootstock/scion, irrigation regime, and Se-NP concentration significantly influenced various physiological parameters. For instance, the highest RWC values were obtained from the 10 ppm Se-NP treatment of 1103 P/CS under well-irrigated conditions (Fig. 3E, Supplementary Material Table 3), while the lowest drought index values under drought stress were observed in the 10 ppm Se-NP treatments for all three rootstocks (Fig. 4C, Supplementary Material Table 3). These findings highlight the importance of considering genotypic variations and the potential for rootstock-mediated effects in response to Se-NP treatments and drought stress.

The effect of Se-NP applications on biochemical parameters

Our findings revealed that drought stress significantly increased leaf surface temperature, drought index, membrane damage index, hydrogen peroxide (H_2O_2), and malondialdehyde (MDA) content across all three rootstock/scion combinations. These findings indicate the detrimental effects of water deficit on cellular membrane integrity and oxidative stress in grapevine saplings. The observed increase in leaf surface temperature under drought stress conditions can be attributed to reduced transpirational cooling due to stomatal closure, which is a plant's defense mechanism to minimize water loss [59]. The drought index and membrane damage index, measured by electrolyte leakage, are indicators of cellular membrane damage and loss of membrane stability, which are commonly observed in plants under water deficit conditions [60, 61]. The accumulation of H_2O_2 and MDA under drought stress is a consequence of increased ROS production and lipid peroxidation, respectively. During drought stress, mitochondria produce more H_2O_2, and the high ROS levels (H_2O_2 and superoxide radicals) can trigger lipid peroxidation, which in turn can act as a signal for the regulation of antioxidant defense systems [62, 63]. The increase in MDA content can be attributed to cellular membrane damage and decreased membrane stability under water-limited conditions [60, 61]. Interestingly, the application of Se-NPs, particularly at 1 and 10 ppm concentrations, significantly reduced leaf surface temperature, membrane damage index, hydrogen peroxide, and MDA content under drought conditions. These results indicate the potential of Se-NPs in mitigating oxidative stress and protecting cellular membranes from drought-induced damage. These findings are consistent with previous studies reporting the roles of Se-NPs in activating antioxidant defense mechanisms, enhancing antioxidant production, and reducing H_2O_2 and MDA accumulation under stress conditions [23, 24, 64]. Furthermore, the application of Se-NPs, particularly at 1 and 10 ppm concentrations, significantly reduced the drought index under water-limited conditions. This finding suggests that Se-NPs can enhance the ability of plants to maintain water balance and mitigate the negative impacts of drought stress. The positive effects of Se-NPs on osmotic adjustment and water homeostasis have been reported in various plant species [64, 65].

The study also revealed that drought stress significantly increased the total phenolic and proline content, whereas Se-NP applications were effective in reducing these parameters under drought conditions. These results are in line with previous reports suggesting the accumulation of osmolytes, such as proline, and phenolic compounds as a defense mechanism in plants under water deficit conditions [66–70]. However, it is noteworthy that conflicting reports exist regarding the effects of abiotic stresses on phenolic content, which may be attributed to differences in experimental conditions, plant species, developmental stages, and the specific phenolic compounds evaluated [71, 72]. The study further revealed that drought stress caused significant reductions in protein content, while Se-NP applications, particularly at 1 and 10 ppm concentrations, effectively increased protein content under both well-irrigated and drought conditions. These findings are consistent with previous reports demonstrating the negative effects of drought stress on protein content [60] and the beneficial role of Se in improving protein synthesis and metabolism [51]. Regarding antioxidant enzyme activities, the study showed that drought stress significantly increased SOD, CAT, and APX activities. However, Se-NP applications caused a significant reduction in SOD, CAT, and APX activities under drought conditions, while increasing SOD and CAT activities under well-irrigated conditions. These results suggest a complex interaction between Se-NPs, drought stress, and antioxidant enzyme activities. The observed increase in antioxidant enzyme activities under drought stress is a common defense mechanism in plants, as these enzymes play crucial roles in detoxifying intracellular free radicals and preventing lipid peroxidation, thereby facilitating efficient photosynthetic activity under stress conditions [73, 74]. The positive effects of Se-NPs on antioxidant enzyme activities and drought tolerance have been reported in various plant species, including maize and ramie [50, 75, 76]. However, the findings of the present study indicate

a complex interplay between Se-NPs, drought stress, and antioxidant enzyme activities, which may be influenced by factors such as plant species, developmental stages, and the specific experimental conditions employed. Further investigations are warranted to elucidate the underlying mechanisms and optimize the use of Se-NPs for enhancing antioxidant defense systems and drought tolerance in grapevines.

General evaluation

The correlation analysis revealed several important insights into the relationships between various physiological and biochemical parameters in grapevine saplings under well-irrigated and drought stress conditions, with and without Se-NP treatments. The strong positive correlation observed between shoot dry weight and fresh weight indicates a close relationship between water content and dry matter accumulation during plant growth. These results suggest that shoot development and growth are strongly influenced by water availability, which is consistent with the well-established role of water in plant physiological processes. Furthermore, the highly positive correlation between root dry weight and shoot dry weight indicates a link between root growth and the growth potential of shoots. This finding highlights the importance of a healthy root system for supporting shoot growth and development, as roots are responsible for water and nutrient uptake from the soil. The positive correlation between RWC and parameters such as leaf number, leaf area, and shoot length suggests that an increase in plant water content enhances growth potential. Conversely, the negative correlation between drought index, membrane damage index, and parameters like leaf area and shoot length indicates that an increase in drought-induced stress damage leads to a reduction in plant growth and development. The relationships between oxidative stress indicators, such as lipid peroxidation, hydrogen peroxide content, and membrane damage index, with various parameters were also highlighted. For instance, the positive correlation between lipid peroxidation and phenolic compound content suggests that an increase in lipid damage triggers the synthesis of secondary compounds, which is a strong defense strategy in plants. Additionally, the high positive correlation between H_2O_2 and APX activity indicates the activation of the antioxidant defense system in plants exposed to drought stress. However, the negative correlation between soluble protein content and lipid peroxidation suggests that an increase in soluble protein levels can reduce cellular lipid damage. Similarly, the strong negative correlation between soluble protein content and H_2O_2 content indicates a decrease in soluble protein levels when plants are exposed to drought stress, reflecting the regulation of protein metabolism and the reorganization of proteins to maintain cellular functions under stress conditions. On the other hand, the principal component analysis (PCA) provided insights into the effects of Se-NP applications on plant growth and drought stress tolerance. The results indicate that the evaluated variables can be strongly explained by the related component analysis, along with the treatments. These findings suggest that Se-NP applications can modulate plant stress responses in different ways and have varying effects on growth. Particularly, the application of Se-NPs at 10 ppm concentration promoted plant growth under drought conditions, while concentrations of 1 and 100 ppm had different effects. These results suggest that NP applications may play a potentially significant role in plant cultivation, which is consistent with previous studies demonstrating the ability of NP applications to modulate plant stress responses and promote growth [50, 75, 76]. The hierarchical clustering heatmap analysis further revealed that the 1103P/CS-DS-10 treatment, which exhibited lower stress parameters and higher growth characteristics, demonstrates the potential of using appropriate NP concentrations and rootstock/scion combinations to enhance stress tolerance in plants under drought conditions. These findings are supported by other studies in the literature, which have reported the potential role of nanoparticle applications in mitigating stress responses and promoting growth in plants under stress conditions [48, 77].

Conclusion

The findings demonstrated that foliar application of Se-NPs in grapevine saplings enhanced their drought tolerance ability by balancing the antioxidant defense system (SOD, CAT, APX enzyme activities and phenolic compound content), increasing proline and protein accumulation, while alleviating oxidative damage by reducing membrane damage index, lipid peroxidation, and hydrogen peroxide production, as well as improving relative water content (RWC), photosynthetic activity (stomatal conductance and SPAD index), and growth parameters. Our results specifically recommend the application of Se-NPs at a concentration of 10 ppm for mitigating stress effects in grapevine saplings under drought stress. However, it was found that the effect of NP application at 1 ppm concentration generally remained limited, while the 100 ppm concentration led to phytotoxic effects, particularly when combined with drought conditions. Our findings further reinforce the concept of nano-enabled agriculture, revealing that these nanomaterials, when applied at appropriate concentrations, could be promising elicitor candidates to alleviate abiotic stress

tolerance. This plant nanobiotechnology approach offers an alternative option for policymakers and farmers, particularly grape growers, to address the existing drought issue in the field and explore semi-arid areas for cultivation. Additionally, it should be noted that safety assessments, such as the effects on non-target organisms, need to be conducted before the application of nanomaterials in grapevines to benefit sustainable agriculture. Future research should comprehensively evaluate the impact of NP applications and investigate the interactions between different NPs, irrigation regimes, and grapevine varieties in more detail. Moreover, molecular analyses are needed to better understand the mechanisms underlying the effects of NPs on plant growth and stress tolerance.

Supplementary Information

The online version contains supplementary material available at https://doi.org/10.1186/s40538-024-00609-6.

Additional file 1.

Acknowledgements
This study was financially supported by The Scientific and Technological Research Council of Turkey (TUBITAK) under the 1002—A Rapid Support Module with the project number "123O608" entitled "Determination of the Effects of Se, SiO_2 and TiO_2 Nanoparticles on the Morphological, Physiological and Biochemical Properties of Grapevine Saplings Against Drought Stress".

Author contributions
S.D., N.K., and O.K., were involved in the investigation, methodology, and conceptualization. S.D., T.K., H.H.V., and O.K handled draft preparation, software, and formal analysis. O.K. was responsible for the original writing and review editing. The visualization was conducted by S.D., N.K., T.K., H.H.V A.K., and O.K. All authors have read and approved the final manuscript.

Funding
The current research has received no funding from agencies in the public, commercial, or not-for-profit sectors.

Availability of data and materials
Requests for materials should be directed to S.D and O.K.

Declarations

Ethics approval and consent to participate
Not applicable.

Consent for publication
Not applicable.

Competing interests
The authors confirm that they have no conflicts of interest with respect to the work described in this manuscript. There are no financial or personal relationships by the authors that could inappropriately influence the work presented.

Author details
[1]Department of Horticulture, Faculty of Agriculture, Yozgat Bozok University, Yozgat, Turkey. [2]Basic Sciences and Health Department, Hemp Research Institute, Yozgat Bozok University, Yozgat, Turkey. [3]Department of Plant Sciences , North Dakota State University, 58102 Fargo, USA. [4]Department of Chemistry, Science and Letters Faculty , Gaziosmanpaşa University, 60250 Tokat, Turkey. [5]Republic of Turkey Ministry of Agriculture and Forestry, Erzincan Horticultural Research Institute, Erzincan, Turkey. [6] Department of Life Sciences, Western Caspian University, Baku 1001, Azerbaijan.

Received: 21 June 2024 Accepted: 9 July 2024
Published online: 05 August 2024

References

1. Pagay V, Furlan TS, Kidman CM, Nagahatenna D. Long-term drought adaptation of unirrigated grapevines (*Vitis vinifera* L.). Theor Exp Plant Physiol. 2022;34:215–25.
2. FAO, 2023. "Food and Agriculture Organization of the United Nations". https://www.fao.org/faostat/en/#data/QCL. Son erişim tarihi: 23 Ocak 2023.
3. IPCC, 2014. Intergovernmental Panel on Climate Change. Climate change. impacts, adaptation and vulnerability: regional aspects. New York: Cambridge University Press; 2014.
4. Fageria, N.K., Baligar, V.C., Clark, R. 2006. Physiology of Crop Production. Food Products Press.
5. Cardone MF, Perniola R, Catacchio CR, Alagna F, Rotunno S, Crupi P, Antonacci D, Velasco R, Ventura M, Bergamini C. "Grapevine adaptation to drought: New candidate genes for the genotype-dependent response", 42nd World Congress of Vine and Wine. BIO Web of Conferences. 2019;15:01016.
6. Calderan A, Sivilotti P, Braidotti R, Mihelčič A, Lisjak K, Vanzo A. Managing moderate water deficit increased anthocyanin concentration and proanthocyanidin galloylation in "Refošk" grapes in Northeast Italy. Agric Water Manag. 2021;246: 106684.
7. Oguz MÇ, Aycan M, Oguz E, Poyraz I, Yildiz M. Drought stress tolerance in plants: Interplay of molecular, biochemical and physiological responses in important development stages. Physiologia. 2022;2:180–97.
8. Ju YL, Yue XF, Min Z, Wang XH, Fang YL, Zhang JX. VvNAC17, a novel stress-responsive grapevine (*Vitis vinifera* L.) NAC transcription factor, increases sensitivity to abscisic acid and enhances salinity, freezing, and drought tolerance in transgenic Arabidopsis. Plant Physiol Biochem. 2020;146:98–111.
9. Balint G, Reynolds AG. Effect of different irrigation strategies on vine physiology, yield, grape composition and sensory profiles of *Vitis vinifera* L. Cabernet-Sauvignon in a cool climate area. Oeno One. 2014;48:269–92.
10. Dry PR, Loveys BR, McCarthy MG, Stoll M. Strategic irrigation management in Australian vineyards. J Int des sciences de la vigne et du vin. 2001;35:129–39.
11. Chaves MM, Zarrouk O, Francisco R, Costa MJ, Santos T, Regalado PA, Rodrigues LM, Lopes MC. Grapevine under deficit irrigation: hints from physiological and molecular data. Ann Appl Biol. 2010;105(5):661–76.
12. Zhang L, Marguerit E, Rossdeutsch L, Ollat N, Gambetta GA. The influence of grapevine rootstocks on scion growth and drought resistance. Theor Exp Plant Physiol. 2016;28(2):143–57.
13. Beslic Z, Pantelic M, Dabic D, Todic S, Natic M, Tesic Z. Effect of vineyard floor management on water regime, growth response, yield and fruit quality in Cabernet Sauvignon. Sci Hortic. 2015;197:650–6.
14. van Leeuwen C, Destrac-Irvine A. Modified grape composition under climate change conditions requires adaptations in the vineyard. Oeno One. 2017;51:147–54.
15. Rienth M, Scholasch T. State-of-the-art of tools and methods to assess vine water status. Oeno One. 2019;53:619–37.
16. Adrees M, Khan ZS, Ali S, Hafeez M, Khalid S, Rehman MZU, Hussain A, Hussain K, Chatha SAS, Rizwan M. Simultaneous mitigation of cadmium and drought stress in wheat by soil application of iron nanoparticles. Chemosphere. 2020;238: 124681.
17. Biju V, Itoh T, Anas A, Sujith A, Ishikawa M. Semiconductor quantum dots and metal nanoparticles: Syntheses, optical properties, and biological applications. Anal Bioanal Chem. 2008;391:2469–95.
18. Cao X, Wang Y, Wang ZL, Tian XL, Han X, Wu D, Yao F, Hui M, Li H, Wang H. Effects of kaolin particle film coatings on the water-saving efficiency and fruit quality of Cabernet Sauvignon (*Vitis vinifera* L.) grape plants in the Ningxia region of China. Hortic Environ Biotechnol. 2023;64:421–35.
19. White JC, Gardea-Torresdey J. Achieving food security through the very small. Nat Nanotechnol. 2018;13:627–9.

20. Kaur N, Sharma S, Kaur S, Nayyar H. Selenium in agriculture: A nutrient or contaminant for crops? Arch Agron Soil Sci. 2014;60:1593–624.
21. Asghari, J., Mahdavikia, H., Rezaei-Chiyaneh, E., Banaei-Asl, F., Amani Machiani, M., Harrison, M.T. 2023. "Selenium nanoparticles improve physiological and phytochemical properties of basil (*Ocimum basilicum* L.) under drought stress conditions", Land, 12, 164.
22. Ikram M, Raja NI, Javed B, Mashwani ZR, Hussain M, Hussain M, Ehsan M, Rafique N, Malik K, Sultana T, Akram A. Foliar applications of bio-fabricated selenium nanoparticles to improve the growth of wheat plants under drought stress. Green Process Synth. 2020;9(1):706–14.
23. Zahedi SM, Moharrami F, Sarikhani S, Padervand M. Selenium and silica nanostructure-based recovery of strawberry plants subjected to drought stress. Sci Rep. 2020;10(1):17672. https://doi.org/10.1038/s41598-020-74273-9.
24. Djanaguiraman M, Belliraj N, Bossmann SH, Vara Prasad PV. High-temperature stress alleviation by selenium nanoparticle treatment in grain sorghum. ACS Omega. 2018;3(3):2479–91. https://doi.org/10.1021/acsomega.7b01934.
25. Ollat N, Geny L, Soyer J. Les boutures fructifères de vigne: validation d, un modèle d, etude du development de la physiologie de la vigne, I Caractèristiques de l'appareil vegetative. J Int des Sciences de la Vigne et du Vin. 1998;32:1–9.
26. Korkmaz N, Ceylan Y, Taslimi P, Karadağ A, Bülbül AS, Şen F. Biogenic nano silver: synthesis, characterization, antibacterial, antibiofilms, and enzymatic activity. Adv Powder Technol. 2020;31(7):2942–50.
27. Fardsadegh B, Vaghari H, Mohammad-Jafari R, Najian Y, Jafarizadeh-Malmiri H. Biosynthesis, characterization and antimicrobial activities assessment of fabricated selenium nanoparticles using Pelargonium zonale leaf extract. Green Process Synth. 2019;8(1):191–8.
28. Cochetel N, Ghan R, Toups HS, Degu A, Tillett RL, Schlauch KA, Cramer GR. Drought tolerance of the grapevine, Vitis champinii cv. Ramsey, is associated with higher photosynthesis and greater transcriptomic responsiveness of abscisic acid biosynthesis and signaling. BMC Plant Biol. 2020;20:55.
29. Earl HJ. A precise gravimetric method for simulating drought stress in pot experiments. Crop Sci. 2003;43:1868–73. https://doi.org/10.2135/cropsci2003.1868.
30. OIV, Descriptors for Grapevine (*Vitis* ssp.) 1997. Descriptors for Grapevine (*Vitis* ssp.). Rome: International Plant Genetic Resources Institute.
31. Geravandi M, Farshadfar E, Kahrizi D. Evaluation of some physiological traits as indicators of drought tolerance in bread wheat genotypes. Russ J Plant Physiol. 2011;58(1):69–75.
32. Yamasaki S, Dillenburg LC. Measurements of leaf relative water content in *Araucaria angustifolia*. Rev Bras Fisiol Veg. 1999;11:69–75.
33. Nayyar H. Accumulation of osmolytes and osmotic adjustment in water-stressed wheat (*Triticum aestivum*) and maize (*Zea mays*) as affected by calcium and its antagonists. Environ Exp Bot. 2003;50(3):253–64.
34. Bates L, Waldren RP, Teare ID. Rapid determination of free proline for water stress studies. Plant Soil. 1973;39:205–7.
35. Kiselev KV, Dubrovina AS, Veselova MV, Bulgakov VP, Fedoreyev SA, Zhuravlev YN. The rol-B gene-induced over production of resveratrol in *Vitis amurensis* transformed cells. J Biotechnol. 2007;128:681–92.
36. Singleton VL, Rossi JR. Colorimetry of total phenolics with phosphomolybdic phosphotungstic acid. Am J Enol Vitic. 1965;16:144–58.
37. Velikova V, Yordanov I, Edreva A. Oxidative stress and some antioxidant systems in acid rain-treated bean plants protective role of exogenous polyamines. Plant Sci. 2000;151:59–66.
38. Lutts S, Kinet JM, Bouharmont J. NaCl-Induced senescence in leaves of rice (*Oryza sativa* L.) cultivars differing in salinity resistance. Ann Bot. 1996;78:389–98.
39. Bradford MM. A rapid and sensitive method for the quantitation of microgram quantities of protein utilizing the principle of protein dye-binding. Anal Biochem. 1976;72:248–54.
40. Mutlu, S. 2009. Salisilik asidin arpada (*Hordeum vulgare* L.) soğuk toleransını sağlama ve apoplastik ile simplastik proteinler üzerine etkilerinin incelenmesi (Doktora Tezi). Atatürk Üniversitesi Fen Bilimleri Enstitüsü, Erzurum.
41. Agarwal S, Pandey V. Antioxidant enzyme responses to NaCl stress in *Cassia angustifoli*. Biol Plant. 2004;48:555–60.
42. Gong Y, Toivonen PMA, Lau OL, Wiersma PA. Antioxidant system level in 'Braeburn' apple in related to its browning disorder. Botanical Bull Academia Sinica. 2001;42:259–64.
43. Nakano Y, Asada K. Hydrogen peroxide is scavenged by ascorbate specific peroxidase in spinach chloroplasts. Plant Cell Physiol. 1981;22:867–80.
44. Basu, S., Ramegowda, V., Kumar, A., Pereira, A. 2016. "Plant adaptation to drought stress", F1000 Faculty Rev-1554, 5, 1554.
45. Wang JY, Xiong YC, Li FM, Siddique KHM, Turner NC. Effects of drought stress on morphophysiological traits, biochemical characteristics, yield, and yield components in different ploidy Wheat: a meta-analysis. Adv Agron. 2017;143:139–73.
46. Hsiao TC. Plant responses to water stress. Annu Rev Plant Biol. 1973;24:519–70.
47. Hellal FA, El-Shabrawi HM, Abd El-Hady M, Khatab IA, El-Sayed SAA, Abdelly C. Influence of PEG induced drought stress on molecular and biochemical constituents and seedling growth of Egyptian barley cultivars. J Gen Eng Biotechnol. 2018;16(1):203–12. https://doi.org/10.1016/j.jgeb.2017.10.009.
48. Nasiri, Y., Asadi, M., Zahedi, S.M., Venditti, A. 2024. "Selenium nanoparticles improved biochemical and physiological properties and antioxidant systems of savoury under drought stress", Natural Product Research, 1–11. https://doi.org/10.1080/14786419.2023.2299303
49. Rady MM, Belal HE, Gadallah FM, Semida WM. Selenium application in two methods promotes drought tolerance in *Solanum lycopersicum* plant by inducing the antioxidant defense system. Sci Hortic. 2020;266: 109290. https://doi.org/10.1016/j.scienta.2020.109290.
50. Jiang C, Zu C, Lu D, Zheng Q, Shen J, Wang H, Li D. Effect of exogenous selenium supply on photosynthesis, Na+ accumulation and antioxidative capacity of maize (*Zea mays* L.) under salinity stress. Sci Rep. 2017;7(7):42039. https://doi.org/10.1038/srep42039.
51. Andrade FR, da Silva GN, Guimarães KC, Barreto HBF, de Souza KRD, Guilherme LRG, Faquin V, Dos Reis AR. Selenium protects rice plants from water deficit stress. Ecotoxicol Environ Saf. 2018;164:562–70. https://doi.org/10.1016/j.ecoenv.2018.08.022.
52. Gholami R, Zahedi SM. Identifying superior drought-tolerant olive genotypes and their biochemical and some physiological responses to various irrigation levels. J Plant Nutr. 2019;42:2057–69.
53. Ahmad R, Waraich EA, Nawaz F, Ashraf MY, Khalid M. Selenium (Se) improves drought tolerance in crop plants: a myth or fact? J Sci Food Agric. 2016;96:372–80.
54. Alyemeni MN, Ahanger MA, Wijaya L, Alam P, Bhardwaj R, Ahmad P. Selenium mitigates cadmium-induced oxidative stress in tomato (*Solanum lycopersicum* L.) plants by modulating chlorophyll fluorescence, osmolyte accumulation, and antioxidant system. Protoplasma. 2018;255(2):459–69. https://doi.org/10.1007/s00709-017-1162-4.
55. Hemmati M, Delkhosh B, Rad AHS, Mohammadi GN. Effect of the application of foliar selenium on canola cultivars as influenced by different irrigation regimes. J Agric Sci. 2019;25(3):309–18. https://doi.org/10.15832/ankutbd.424899.
56. El-Batal AI, Sidkey NM, Ismail A, Arafa RA, Fathy RM. Impact of silver and selenium nanoparticles synthesized by gamma irradiation and their physiological response on early blight disease of potato. J Chem Pharm Res. 2016;8(4):934–51.
57. Hernández-Hernández H, Quiterio-Gutiérrez T, Cadenas-Pliego G, Ortega-Ortiz H, Hernández-Fuentes AD, Cabrera de la Fuente M, Valdés-Reyna J, Juárez-Maldonado A. Impact of selenium and copper nanoparticles on yield, antioxidant system, and fruit quality of tomato plants. Plants. 2019;8(10):355. https://doi.org/10.3390/plants8100355.
58. Adebayo AH, Yakubu OF, Bakare-Akpata O. Uptake, metabolism and toxicity of selenium in tropical plants. In importance of selenium in the environment and human health", London: IntechOpen; 2020.
59. Rehman SU, Bilal M, Rana RM, Tahir MN, Shah MKN, Ayalew H, Yan G. Cell membrane stability and chlorophyll content variation in wheat (*Triticum aestivum*) genotypes under conditions of heat and drought. Crop Pasture Sci. 2016;67(7):712–8. https://doi.org/10.1071/CP15385.
60. Liang Y, Wei G, Ning K, Li M, Zhang G, Luo L, Zhao G, Wei J, Liu Y, Dong L, Chen S. Increase in carbohydrate content and variation in microbiome are related to the drought tolerance of *Codonopsis pilosula*. Plant Physiol Biochem. 2021;165:19–35. https://doi.org/10.1016/j.plaphy.2021.05.004.

61. Ghaffari H, Tadayon MR, Nadeem M, Cheema M, Razmjoo J. Proline-mediated changes in antioxidant enzymatic activities and the physiology of sugar beet under drought stress. Acta Physiol Plant. 2019;41(2):1–13. https://doi.org/10.1007/s11738-019-2815-z.
62. Tartoura KA. Alleviation of oxidative-stress induced by drought through application of compost in wheat (*Triticum aestivum* L.) plants. Am J Environ Sci. 2010;9:208–16.
63. Shanazari M, Golkar P, Mirmohammady Maibody AM. Effects of drought stress on some agronomic and bio-physiological traits of *Triticum aestivum*, Triticale, and Tritipyrum genotypes. Arch Agron Soil Sci. 2018;64(14):2005–18. https://doi.org/10.1080/03650340.2018.1472377.
64. Jóźwiak W, Politycka B. Effect of selenium on alleviating oxidative stress caused by a water deficit in cucumber roots. Plants. 2019;8(7):217. https://doi.org/10.3390/plants8070217.
65. Thuc LV, Sakagami JI, Hung LT, Huu TN, Khuong NQ, Vu Vi LL. Foliar selenium application for improving drought tolerance of sesame (*Sesamum indicum* L.). Open Agric. 2021;6(1):93–101. https://doi.org/10.1515/opag-2021-0222.
66. Wu HH, Zou YN, Rahman MM, Ni QD, Wu QS. Mycorrhizas alter sucrose and proline metabolism in trifoliate orange exposed to drought stress. Sci Rep. 2017;7:42389.
67. Chung IM, Kim JJ, Lim JD, Yu CY, Kim SH, Hahn SJ. Comparison of resveratrol, SOD activity, phenolic compounds and free amino acid in Rehmannia glutinose under temperature and water stress. Environ Exp Bot. 2006;56:44–53.
68. Gharibi S, Sayed Tabatabaei BE, Saeidi G, Hossein Goli SA. Effect of drought stress on total phenolic, lipid peroxidation, and antioxidant activity of Achillea species. Appl Biochem Biotechnol. 2015;178:796–809. https://doi.org/10.1007/s12010-015-1909-3.
69. Tripathi P, Rabara RC, Shulaev V, Shen QJ, Rushton PJ. Understanding water-stress responses in soybean using hydroponics system-a systems biology perspective. Front Plant Sci. 2015;6:1145. https://doi.org/10.3389/fpls.2015.01145.
70. Faghih S, Zarei A, Ghobadi C. Positive effects of plant growth regulators on physiology responses of Fragaria × ananassa cv. 'Camarosa' under salt stress. Int J Fruit Sci. 2019;19(1):104–14. https://doi.org/10.1080/15538362.2018.1462291.
71. Amarowicz R, Weidner S, Wojtowicz I, Karmac´, M., Kosin´ska, A., Rybarczyk, A. Influence of low-temperature stress on changes in the composition of grapevine leaf phenolic compounds and their antioxidant properties. Funct Plant Sci Biotechnol. 2010;4:90–6.
72. Krol A, Amarowicz R, Weidner S. Changes in the composition of phenolic compounds and antioxidant properties of grapevine roots and leaves (*Vitis vinifera* L.) under continuous of long-term drought stress. Acta Physiol Plant. 2014;36:1491–9.
73. Analin B, Mohanan A, Bakka K, Challabathula D. Cytochrome oxidase and alternative oxidase pathways of mitochondrial electron transport chain are important for the photosynthetic performance of pea plants under salinity stress conditions. Plant Physiol Biochem. 2020;154:248–59. https://doi.org/10.1016/j.plaphy.2020.05.022.
74. Xie X, He Z, Chen N, Tang Z, Wang Q, Cai Y. The roles of environmental factors in regulation of oxidative stress in plant. BioMed Res Int. 2019;1:9732311–25. https://doi.org/10.1155/2019/9732325.
75. Zeeshan M, Hu YX, Iqbal A, Salam A, Liu YX, Muhammad I, Ahmad S, Khan AH, Hale B, Wu HY, Zhou XB. Amelioration of ASV toxicity by concurrent application of ZnO-NPs and Se-NPs is associated with differential regulation of photosynthetic indexes, antioxidant pool and osmolytes content in soybean seedling. Ecotoxicol Environ Saf. 2021;225: 112738. https://doi.org/10.1016/j.ecoenv.2021.112738.
76. Gholami S, Dehaghi MA, Rezazadeh A, Naji AM. Seed germination and physiological responses of quinoa to selenium priming under drought stress. Bragantia. 2022. https://doi.org/10.1590/1678-4499.20210183.
77. Ahmed KBM, Khan MMA, Shabbir A, Ahmad B, Uddin M, Azam A. Comparative effect of foliar application of silicon, titanium and zinc nanoparticles on the performance of vetiver-a medicinal and aromatic plant. Silicon. 2023;15:153–66. https://doi.org/10.1007/s12633-022-02007-9.

Publisher's Note

Springer Nature remains neutral with regard to jurisdictional claims in published maps and institutional affiliations.